Faculdade de Engenharia da Universidade do Porto

SHORT-TERM FORECASTING OF PHOTOVOLTAIC POWER PLANTS

Pedro Henrique Cardeal Serra

Thesis written in the ambit of Master in Electrical and Computers Engineering
Major in Energy

Advisor: José Nuno Fidalgo (Dr.)

Co-Advisor: Ricardo Bessa (Dr.)

January 2014

Abstract

Solar power is the biggest source of energy that humanity has access to. Although the solar energy is not the most used source of renewable energy its share in the global power production has been increasing. Solar power forecasting is a key tool for the integration of this kind of energy production into the grid, enabling an efficient management and control of the power generation system. Thus, the aim of the present thesis is the development of a solar power forecasting method.

There are several Numerical Weather Predictions (NWP) variables which can influence the solar power production of a PV panel, and were tested in this work; this includes variables such as Global Horizontal Irradiance, Direct Normal Irradiance, and Cloudiness, among others.

This thesis presents a short-term forecasting method for photovoltaic power production, in this specific case a forecast is made for a time span of 72 hours ahead. This forecasting method is based on Extreme Learning Machines, a relatively new statistical method. The present method uses a combination of NWP and series of past values, thus being classified as a hybrid method.

The forecast for the time span is made for each hour separately and has the capacity to start at whatever hour is suited for the electricity market or the power producer.

The performance of the forecasting method is rated by an error measure process, the results were better for the first 5 hours of the time span beginning below 6% for the first hour and steadily rising to around 9%, once they use series of the past power production values as input, for the span of the hours 6-72 the Numerical Weather Predictions were found to be a more relevant input with an error always rounding 11%.

Keywords: Solar Power, Extreme Learning Machines, Photovoltaic Forecasting, Numerical Weather Predictions, Irradiance, Renewable Energies.

Resumo

A energia solar é a maior fonte de energia a que a humanidade tem acesso. Apesar de a energia solar não ser a fonte de energia renovável mais utilizada a sua quota-parte na produção global de energia tem vindo a subir. A previsão fotovoltaica é um instrumento chave para a integração da produção das energias renováveis na rede, fazendo com que seja possível uma gestão e controlo mais eficiente do sistema electroprodutor. Assim, o principal foco da presente dissertação é o desenvolvimento de um modelo de previsão fotovoltaica.

Existem várias variáveis Numerical Weather Predictions (NWP) que podem influenciar a produção de um painel fotovoltaico e que foram testadas no presente trabalho; isto inclui variáveis tais como irradiância global horizontal, irradiância direta e nebulosidade, entre outras.

Esta tese apresenta um método de previsão da produção fotovoltaica a curto-prazo, mais especificamente, uma previsão é feita para um período de 72 horas à frente. Este método de previsão é baseado em Extreme Learning Machines, um método estatístico relativamente recente. O presente método combina NWP e séries de valores passados, sendo assim classificado como um método hibrido.

A previsão é feita em separado para cada uma das horas do espaço temporal e tem também a capacidade de começar a qualquer hora do dia, de maneira a ser mais conveniente para o mercado ou para o produtor.

A performance do método de previsão desenvolvido é avaliado com um procedimento de medido do erro, os resultados foram melhoras para as primeiras 5 horas do horizonte de previsão, começando abaixo dos 6% para a primeira hora do horizonte subindo até por volta dos 9% para a quinta hora, uma vez que estas usam valores passados para a sua previsão, para o horizonte das 6-72 horas as NWP revelaram-se variáveis de entrada de maior importância do que para as primeiras horas tendo assim um erro associado que ronda os 11%.

Palavras-chave: Energia Solar, Extreme Learning Machines, Previsão Fotovoltaica, Numerical Weather Predictions, Irradiância, Energias renováveis.

Acknowledgements

This moment offers the opportunity to thank to every person and institution which, directly or indirectly, helped and contributed to the elaboration of the present thesis.

Firstly, to my advisors Dr. José Nuno Fidalgo and Dr. Ricardo Bessa, for all their help and experience which proved to be of great value in the course of the present work. Also, for the availability demonstrated in the long hours of reunions and discussions throughout the semester. Without their guidance this thesis would not have been possible.

To the opportunity to do this thesis, a note of thanking is due to INESC Porto (Instituto de Engenharia de Sistemas e Computadores do Porto).

To all my colleagues and friends who accompanied me during this stage of my life, for the support, friendship and companionship demonstrated during not only the long hours of study and work, but also outside college.

To my family who provided the best conditions for my education and academic path as well as my personal and professional realization.

Lastly, but not at all less important, to my girlfriend Maria, who supported me in every moment of this last journey as a student and whose constant presence and encouragement always kept me focused.

This work was developed in the framework of the BEST CASE project ("NORTE-07-0124-FEDER-000056") financed by the North Portugal Regional Operational Programme (ON.2 – O Novo Norte), under the National Strategic Reference Framework (NSRF), through the European Regional Development Fund (ERDF), and by national funds, through Fundação para a Ciência e a Tecnologia (FCT). It was also developed within FCT projects «SMAGIS – PTDC/SEN-ENR/113094/2009» and «DYMONDS – CMU-PT/SIA/0043/2009».

“Chaos is the score upon which reality is written.”
-Henry Miller

Contents

Figure List

Table List

Abbreviations and Symbols

Abreviation List

ANN	Artificial Neural Network
AR	Autoregression
ARIMA	Autoregressive integrated mean average
ARMA	Autoregressive mean average
BP	Back Propagation
DEEC	Departamento de Engenharia Eletrotécnica e de Computadores
DHI	Diffuse Horizontal Irradiance
DNI	Direct Normal Irradiance
ECMWF	European Centre for Medium-Range Weather Forecasts
ELM	*Extreme Learning Machines*
FEUP	Faculdade de Engenharia da Universidade do Porto
GHI	Global Horizontal Irradiance
GTS	Global Telecommunication System
LS	Least Square
LS-SVM	Least Square Support Vector Machine
MAE	Mean Average Error
MLP	Multilayer Perceptron
MSG	Meteosat Second Generation
NDFD	National Digital Forecast Database
NN	Neural Network

NWP	Numerical Weather Predictions
PSVM	Proximal Support Vector Machine
PV	Photovoltaic
PWL	Piece-Wise Linear
RAMS	Regional Atmospheric Modeling System
RBF	Radial Basic Function
RBF	Radial Basis Function
RMSD	Root Mean Square Deviation
RMSE	Root Mean Square Error
SLFN	Single-layer Feedforward Network
SVD	Single Value Decomposition
SVM	Support Vector Machines
SVR	Support Vector Regression
TBF	Triangular Basis Function
TDNN	Time Delay Neural Network
VC	Vapnik-Chervonenkis
WMO	World Meteorological Organization

Symbol List

α	Elevation angle
δ	Declination angle
φ	Latitude of the current location
α_s	Solar azimuth
Υ_s	Solar elevation angle
α	Collector azimuth
β	Collector elevation angle
y_t'	Differenced series
β	Vector of the output weights between the hidden layer and the output node

$h(x)$	Output vector of the hidden layer
H	Hidden layer output matrix
$H^{\dagger}$	Moore-Penrose generalized inverse matrix
$P_{t_{-1}}$	Produced power one hour before the forecasting
P_{dayb}	Produced power one day before the hour for which the forecast is made
K	Hour which will be forecasted
D	Day for which the forecast will be made
P_t	Solar Power
P_t^{CS}	Clear sky solar power
τ_t	Normalized solar power
$P_{t,k}$	Measured power production
$\hat{P}_{t,k}$	Forecasted power production
G	Global Irradiance
G_{cs}	Clear sky global irradiance
τ_c	Transmissivity of the clouds
I_0	Extraterrestrial irradiance
τ_a	Total sky transmissivity in clear sky
p	Solar power
p_{cs}	Clear sky power
$\hat{p}_t^{cs}$	Clear sky estimated solar power

Chapter 1

Introduction

This thesis was developed in the ambit of the Master in Electrical and Computers Engineering at Faculdade de Engenharia da Universidade do Porto (FEUP).

The renewable energies are increasingly earning its share in the energetic outlook, even getting at times bigger stakes than traditional energy sources, such as fossil and nuclear, e.g. in Portugal during 2013 there were some days of 100% renewable energy output [6]. With its increasingly demand for energy, humanity needs to invest in this type of power sources and solar power is potentially the biggest one we have access to, as can be seen in Figure 1.1.

In the present thesis a forecasting method for photovoltaic micro-generation is developed using forecasting up to 72 hours ahead using Extreme Learning Machines (ELM) which allows non-linear relationships between power production and numerical weather predictions (NWP). The data used is from a real source located in southern Italy, having, therefore, similar latitude to Portugal.

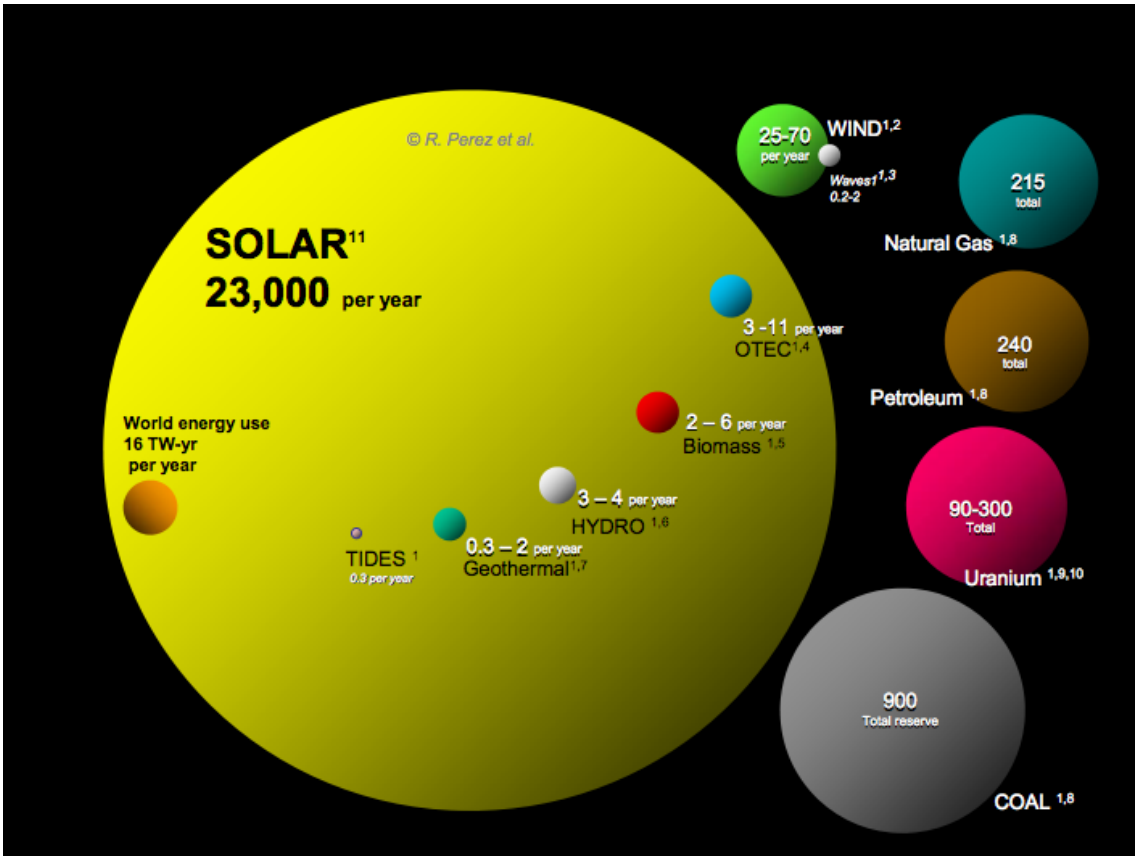

Figure 1.1 - Proportions between traditional energy sources and renewable energy sources [4]

1.1.Motivation

Throughout history, especially since the industrial revolution the energetic demand of populations has been exponentially increasing, making the meeting of those demands a huge problem that governments are facing. The eminence of fossil energy sources depletion as well as the United Nations' pressures concerning greenhouse gases emissions through the Kyoto protocol, have been forcing a turn of investments into renewable energy sources such as photovoltaic and aeolian. The investments in this energy sources have been increasing for the great length of the last decade with a little decrease in 2012, as can be seen in Figure 1.2 and Figure 1.3, the appointed reason being due to the difficult global financial environment that has affected many sectors and many investors are not in a disposition to risk much funds also due to the governments energy policy reforms [8]. Also, the prices of the solar modules have been falling with the evolution of the technology, which can explain, in addition, the fall of the investments.

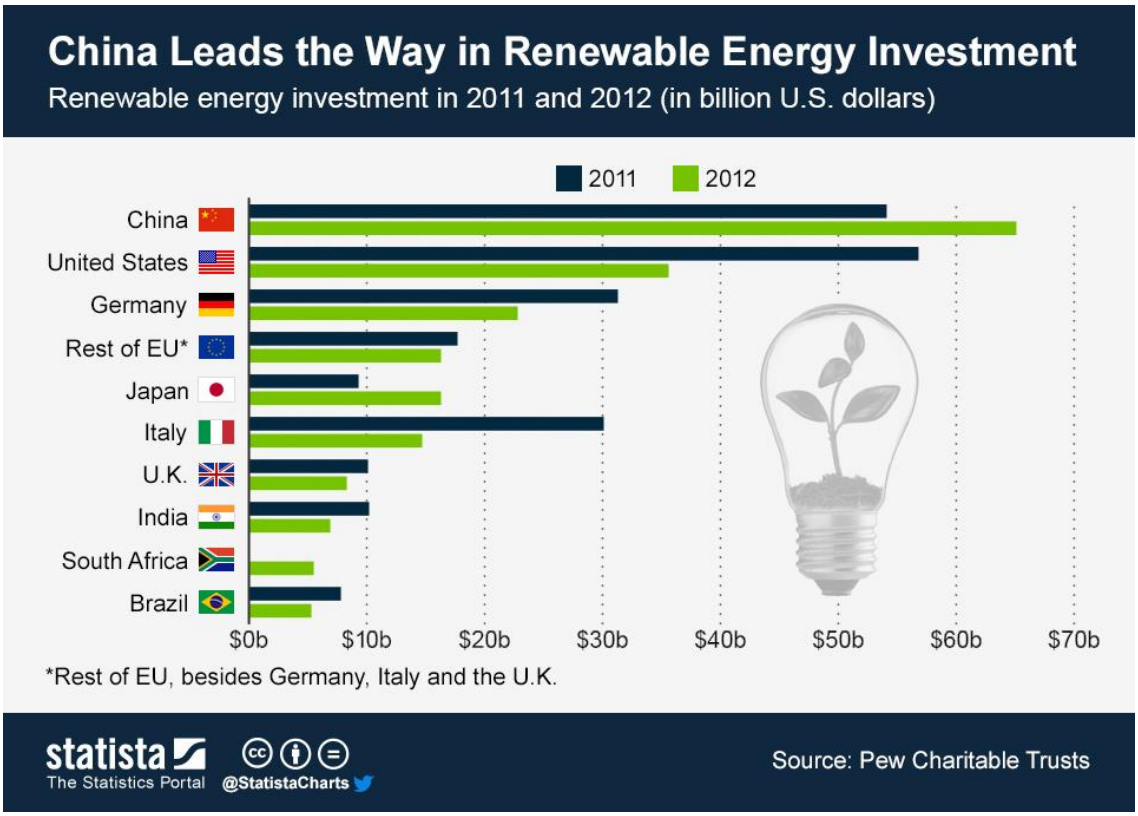

Figure 1.2 - Global investments in renewable energy [7]

The focus of the present thesis resides in solar power forecasting which has an insurmountable capability as seen above in Figure 1.1. Especially in countries like Portugal and Italy which have an annual irradiance considerably high (Figure 1.4), that should be an encouragement for increasing investments. In the latest years the governments have been funding renewable energy production aiming to achieve Kyoto's protocol commitments as well as reducing their dependency from fossil energy sources.

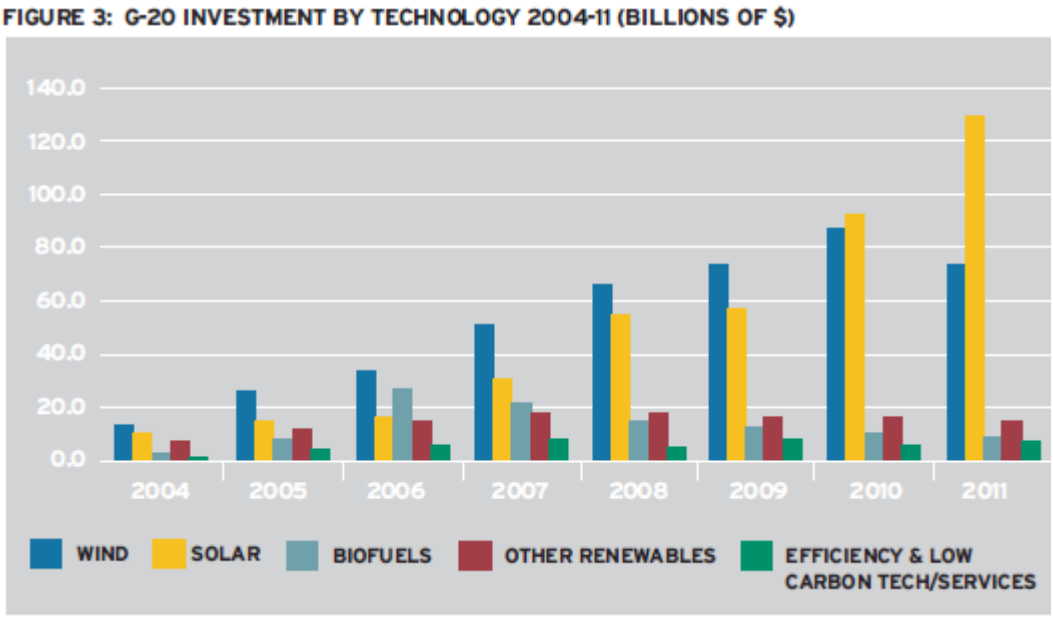

Figure 1.3 - Investment by technology 2004-2011 [80]

It is believed that the photovoltaic energy is about to emerge and gain prominence in the coming years, as can be seen in Figure 1.5 the installed capacity worldwide in 2013 is about 35GW, while estimations for 2020 are above 70GW, it also can be seen that Europe and the Asiatic countries from the zone of Pacific Ocean are the main contributors to this statistic [9].

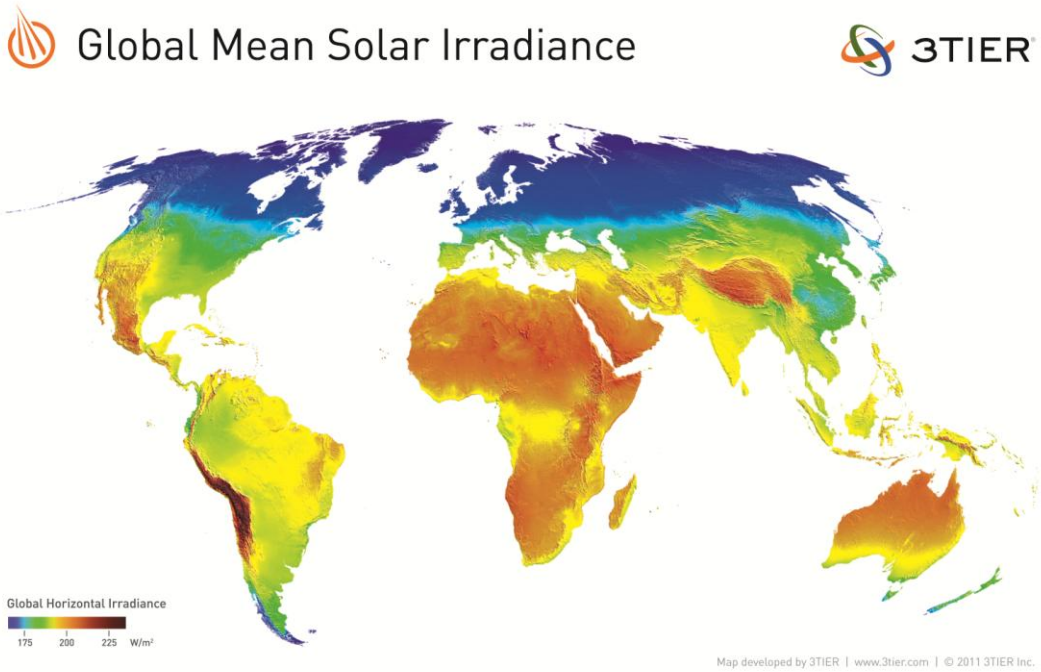

Figure 1.4 - Global mean solar irradiance [10]

Aside from ecological problems governments have been facing, another issue is the fairness between the incentives given to renewable energy producers and competitive prices. These incentives are necessary in order to galvanize and help the development of this kind of power producers.

Also, some countries have managed to create an energy market system, some markets even comprise several nations e.g. the MIBEL including Portugal and Spain, the forecasts are extremely important for the markets as a tool, as will be seen later in the following section. The MIBEL is the platform where all electricity concerning Iberia is transacted setting the prices for every hour of the following day. The daily market session is made at 11 a.m. Portuguese time. The hourly market prices are established by crossing both the selling and buying offers by every agent able to operate in that market. Each offer must point the day and hour for which it is making an offer, as well as the corresponding price and power. The price is found by a process wherein the selling offers are organized in crescent order by price while the buying offers are organized in descent order by price for each hour of the day, and then the market price is given by the point where both curves graphically cross each other. This means the price is the same for every agent who takes part in the auction [5].

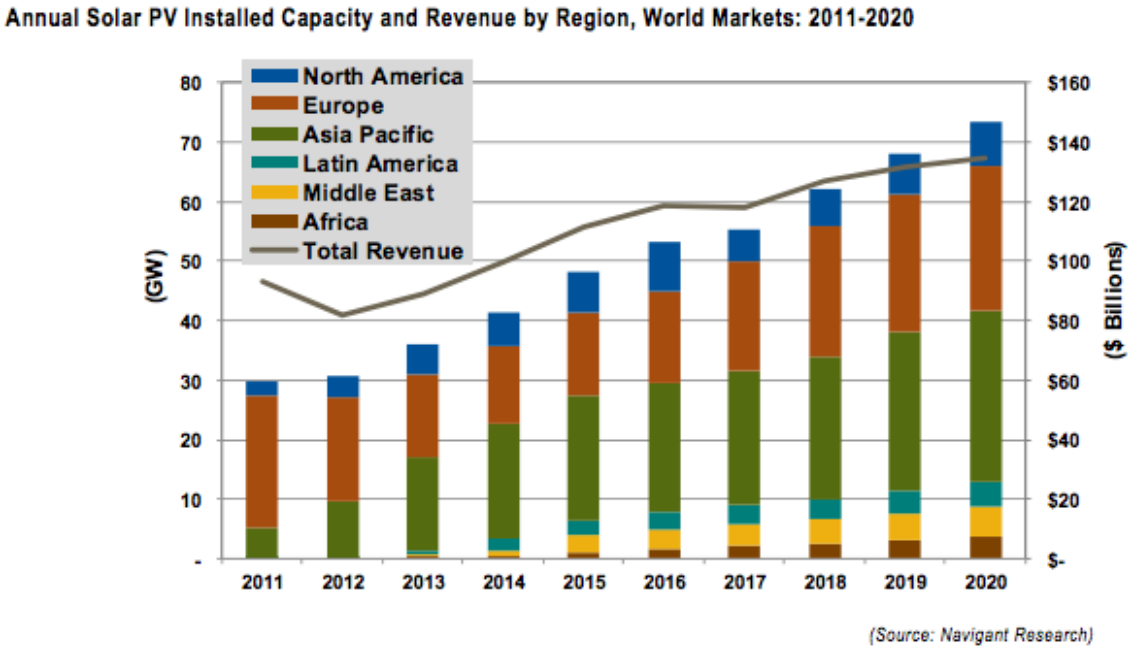

Figure 1.5 - Projections for annual solar PV capacity and revenue [9]

1.2. Relevance of Forecasts

The relevance of renewable energies has been rising substantially in the last two decades, and this growth is expected to persist in the current in the next years, headed by Aeolian and Photovoltaic energies. The volatility of this kind of energy brings out a new problem: If the energy sources cannot be tamed, how can its output be controlled so it can be safely used? The answer to this question has been partly given by the power production forecasts, which can help to greatly diminish a number of issues:

- Great variability in weather sources, e.g., wind and sun;
- The need for a great service quality by the grid and power production;
- The more renewable energy sources the more vulnerable is the system;
- Power markets demand the anticipation of production quantities of each producer;
- The need for system reserves planning;
- Planning interconnections between different grids [2], [12].

Because of the aforementioned reasons it is extremely important that the technologies used in forecasting, keep developing and increasing its performance because they are fundamental to the efficiency of the system and thus, to mankind as well.

Energy efficiency and conservation are important measures that should be considered in conjunction with PV systems. These systems provide a buffer against rising energy prices, and

the presence of an on-site battery bank can supply electricity during utility power outages. Solar power can also help make a difference in the way that we address climate change and the impact on the environment.

There are several ranges of forecasting:

- Long-term forecasting, which is used for an horizon of 5 years up to 25, it is important for grid expansion planning, creating good conditions for short-term expansions;
- Mid-Term forecasting, which is used for an horizon of a few months up to a few years, it is important for financial and expansion planning and maintenance programming;
- Short-term forecasting is used for a horizon of a few hours up to few weeks and it is used for the operation of the grid in short-term [11].

Another important parameter of forecasts is the spatial load forecasting, i.e., the service area of the power producer. The forecasts in this case are important for financial planning, and are often based on macroeconomic aspects, commercial info and time series. This type of forecasting is usually simple because of the great availability of information, internal and external [11];

There are several forecasting models and techniques which range from regression models passing by stochastic models of time series to computational intelligence, which includes artificial neural networks (ANN) that are the foundation for this dissertation. The neural type of ANN used in this work is known by ELM (Extremely learning machines) and it will be presented later on in this document. The forecasting models used in the present work use NWP (Numerical Weather Predictions) as a ground base, and it can include, e.g., Irradiation, Temperature, Solar altitude, Wind speed [11].

1.3. Objectives

The intention of the present thesis is to create a model for short-term forecasting (i.e. up to 72 hours ahead), using auto-learning techniques, of Photovoltaic power plants. The main objective consists in applying innovative concepts based on Extreme Learning Machines (ELM) with variable coefficients, allowing the modelization of non-linear relations between the power plant production and Numerical Weather Predictions (NWP).

The experimentation with several different activation functions is also an integrant part of this thesis in order to understand its effects on the results and to discover which activation function provides better results.

1.4. Structure

The present thesis is constituted by six chapters, being the present chapter dedicated to the introduction of the proposed problem.

The second chapter presents a review of the background of PV systems. It starts by a short introduction about photovoltaic power systems and its constituents. Follows a presentation of the most common weather variables used In PV power output forecasting, such as Global Horizontal Irradiance or Direct Normal Irradiance.

The third chapter is dedicated to the presentation of the State of the Art, and does an overview of various forecasting models which are commonly used for PV power output forecasting. In the end of the chapter some final remarks about the study are made.

The fourth chapter describes the methodology used in this work. This includes the presentation in some degree of detail of the ELM technique, which is a main factor for the development of the work that led to the elaboration of the present document as well as other statistical methods. Also, it is made a comparison between the ELM and these other statistical methods. The data treatments techniques utilized in the development of this work are also presented in this chapter as well as the forecasting model layout.

The fifth chapter presents the discussion and results of this work. A deep insight over the used Numerical Weather Predictions is also given. In addition, an overview of the error measures used in the course of the method is given. Finally, the results are presented and discussed.

The sixth chapter presents the conclusions drawn with this work. A critical analysis is also made. Lastly, some options of future work are presented.

Chapter 2

Background

This chapter presents some aspects of photovoltaic systems. Also, some of the typical photovoltaic power forecasting methods are presented. An insight over the most influential Numerical Weather Predictions for PV forecasting is provided as well.

2.1. Photovoltaic Systems

Photovoltaic (PV) systems are used to convert sunlight to electricity. They are a safe, reliable, low-maintenance source of solar electricity that produces no on-site pollution or emissions. PV systems incur few operating costs and are easy to install on most houses. These systems fall into two main categories – off-grid and grid-connected. The "grid" refers to the local electric utility's infrastructure that supplies electricity to houses and businesses. Off-grid systems are installed in remote locations where there is no utility grid available.

Internationally, utility grid-connected PV systems represent the majority of installations, growing at a rate of 20-30% annually. However, the number of grid-connected systems continues to grow because many of the barriers to interconnection have been addressed through the adoption of harmonized standards and codes. In addition, policies supporting grid interconnection of PV power have encouraged a number of building-integrated PV applications [13].

With the rising of electricity costs, concerns to the reliability of the continuous service delivery and increased environmental awareness of homeowners, the demand for residential PV systems is increasing [13].

Simply put, PV systems are like any other electrical power generating systems. However, the principles of operation and interfacing with other electrical systems remain the same, and are guided by a well-established body of electrical codes and standards.

Although a PV array produces power when exposed to sunlight, a number of other components are required to properly conduct, control, convert, distribute, and store the energy produced by the array.

Depending on the functional and operational requirements of the system, the specific components required may include major components such as DC-AC power inverter, battery bank, system and battery controller, auxiliary energy sources and sometimes the specified electrical load. In addition, an assortment of balance of system hardware, including wiring, over current, surge protection and disconnect devices, and other power processing equipment. Figure 2.1 shows a basic diagram of a PV system and the relationship of individual components [14].

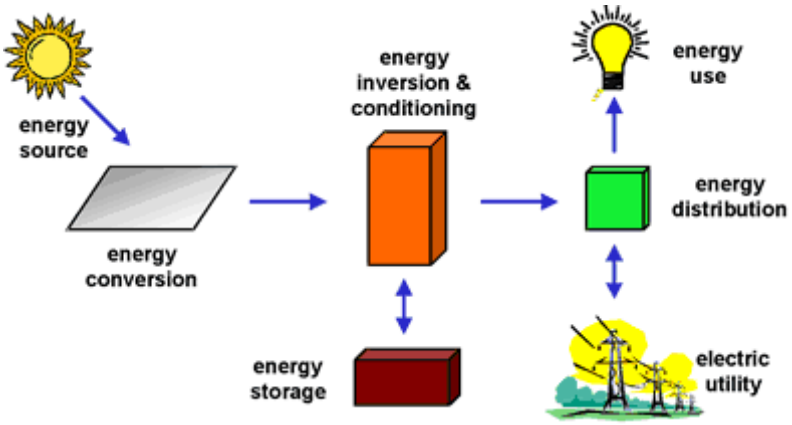

Figure 2.1 - Major PV system components [14]

Batteries are often used in PV systems for the purpose of storing energy produced by the PV array during the day, and to supply it to electrical loads as needed. This happens most often when it's a non grid-connected PV system, although grid-connected systems may include a battery bank.

The most critical component of any PV system is the PV module, which is composed of a number of interconnected solar cells. PV modules are connected together into panels and arrays to meet various energy needs, as shown in Figure 2.2 [13].

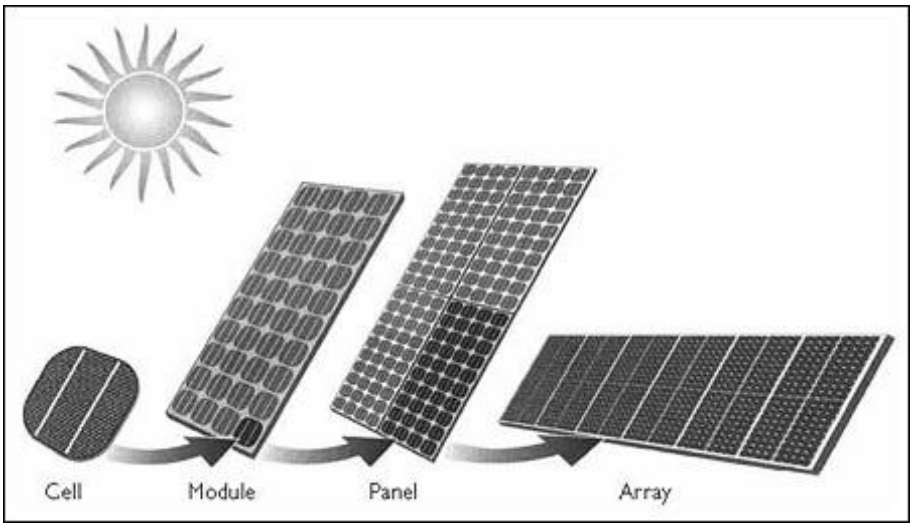

Figure 2.2 - Schematics of PV array components [13]

There are several factors that can influence the output (energy production) of a PV system, although the most important factors are the irradiation and cell temperature. The current produced in modules is linearly linked to the light intensity, thus when irradiance rises the produced electricity will rise as well. Another important factor is the cell temperature, i.e., the rise of cell temperature decreases the efficiency of the module, preventing it to function at maximum power [15]. Another factor to be considered in the phase of panel installation is the wind speed which is important, for accounting the mechanical forces that the array is subjected to.

The knowledge of the exact location of the sun is indispensable for determining the radiation data and the power produced by solar installations. The location of the sun can be defined anywhere by its height and azimuth. In solar energy fields the South is usually referred as α=0º. The negative values are attributed to the East angles (α=-90º) and the positives are attributed to West angles (α=90º).

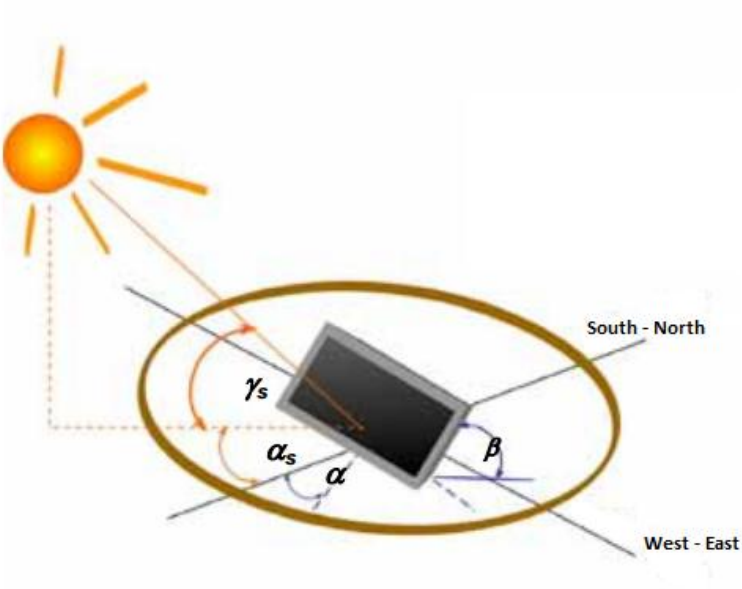

Figure 2.3 - Angle representation following solar techniques [16]

α_s is the solar azimuth, $\gamma_s$is the solar elevation angle, α is the collector azimuth and β is the collector elevation angle [16].

The quantity of solar radiation captured by a surface is maximized when the panel surface is perpendicular to the radiation. This fact is related to the angular absorption variation and to the reflection, as well as to the path followed by the radiation. The inclination of the PV array should optimize the capture of the solar radiation, accounting on elevation and solar azimuth throughout the year, as can be seen in Figure 2.4.

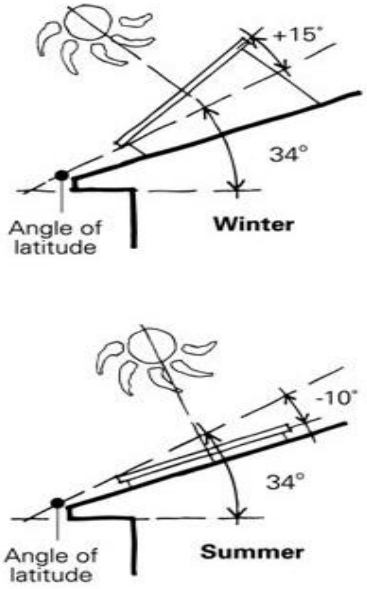

Figure 2.4 - Winter and Summer panel inclinations[17]

2.2.Numerical Weather Predictions

A wide variety of weather phenomena can be analyzed and predicted by several different types of numerical weather prediction models. The numerical weather predictions used for certain kinds of forecasting differ from case to case, e.g., for photovoltaic systems forecasting, the wind speed is not a variable as relevant as global horizontal irradiance, as opposed to wind power forecasting, which takes it as its most important variable. Also, there is a number of variables that may or may not be of importance for some kinds of forecasting models, and they have to be tested so a decision on its inclusion on the forecasting method or not may be responsibly taken.

In this section the available numerical weather predictions for this case are explained, and then discussed for a conclusion on its addition to the model or not is reached.

2.2.1. *GHI – Global Horizontal Irradiance*

The total solar radiation reaching the surface of the earth can be represented in several different ways. Global Horizontal Irradiance (GHI) is the quantity of short wave irradiance falling on the surface of the earth or a surface horizontal to the ground. The GHI is particularly interesting to photovoltaic installations and is composed by both Direct Normal

Irradiance (DNI) and Diffuse Horizontal irradiance (DHI). DNI is solar radiation directly applied to earth coming in a straight line from the position of the sun in the sky. DHI is solar radiation which has been scattered by molecules and particles in the atmosphere and comes in the same amount from all directions. On a cloudy day, most of the solar irradiance received by the earth's surface comes from DHI, while on a clear day, it will mostly come from DNI [44] [45].

The most common instrument to measure GHI is a pyranometer which has a viewing angle of 180° (hemispherical). The trademark of the pyranometer is a true cosine response to incident angle, i.e. its response to a solar beam is proportional to the cosine of the incident angle of the beam. Most pyranometers utilize a thermopile sensor to sense the incoming beams of light. GHI may also be measured with a photovoltaic reference cell, which has a spectral sensitivity and generally will not reveal true cosine response.

If the GHI cannot be directly measured, it may be calculated from DNI and DHI using the subsequent equation [45]:

$$GHI = DHI + DNI \times \cos(\theta_Z)$$

In Figure 2.5 both the factors by which the Global Horizontal Irradiance is composed can be seen:

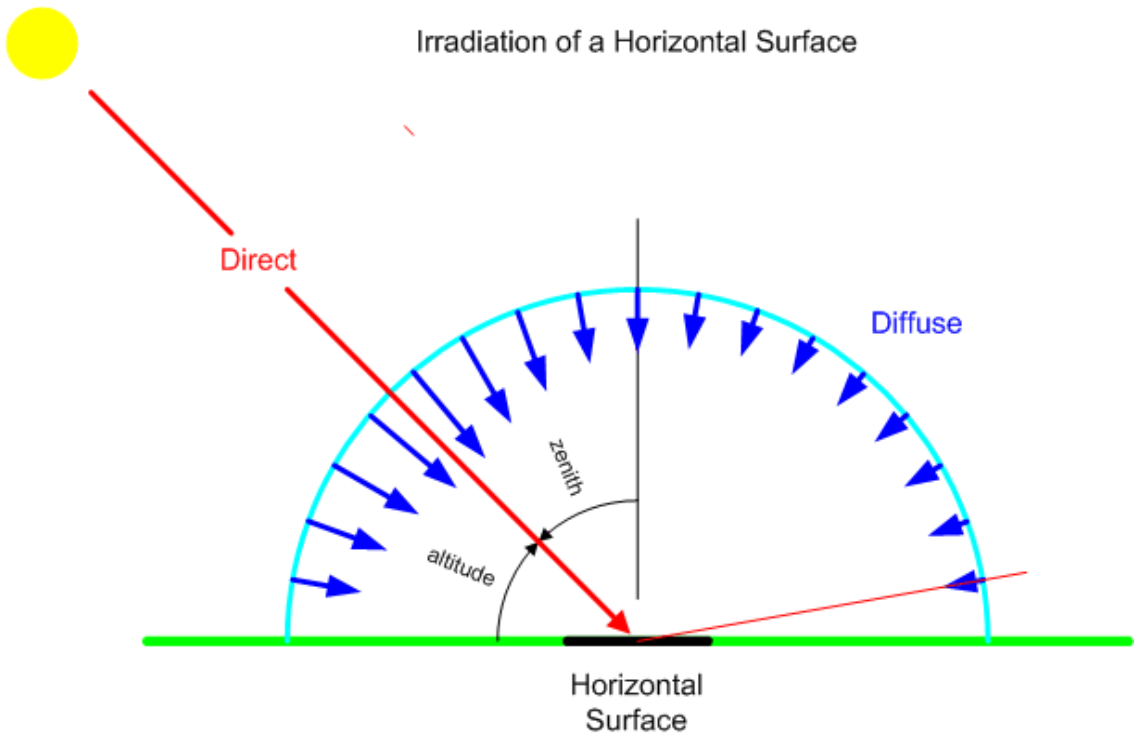

Figure 2.5 – Irradiation of a Horizontal Surface [46]

2.2.2. *DNI – Direct Normal Irradiance*

Direct Solar Irradiance, also known as Direct Normal Irradiance (DNI) is a measure of the rate of solar energy arriving at the Earth's surface directly from the Sun's direct light beam, on a plane perpendicular to the beam, and usually is measured by a pyrheliometer mounted on a solar tracker. This tracker guarantees that the sun beam is always directed into the pyrheliometer field of view, during the day time. The pyrheliometer has a field of view of 5º. In order to use this measure for comparison with global and diffuse irradiances, it is required to obtain the horizontal element of the direct solar irradiance. This is obtained by multiplying the direct solar irradiance by the cosine of the Sun's zenith angle [47].

To maximize the quantity of irradiance received by a surface it is needed to keep it normal to the incoming radiation. This quantity is of particular interest to concentrating solar thermal installations and installations that track the position of the sun [48].

Figure 2.5 illustrates these concepts.

2.2.3. *Temperature*

Temperature can be defined as the measure of hotness or coldness of an object or of the environment that can be measure by using a thermometer [71]. In what concerns forecasting, temperature usually uses Kelvin as a unit, but it can also be measure in Celsius or in Fahrenheit.

Temperature is mostly important for photovoltaic forecasting because of the functioning of the panels, i.e., if the temperature is too high, the photovoltaic panels will start malfunctioning, which lowers their efficiency and consequently is bad for power production. When the opposite occurs, in certain cases, the panels can show a better performance due to the low temperature provided by the environment. So, although it is not a factor as relevant as Global Horizontal Irradiance or Direct Normal Irradiance for the forecasting, temperature can, in certain occasions, be important.

2.2.4. *Cloudiness*

Seen from space, Earth is a blue planet strongly marked by white cloud structures. By reflecting sunlight, blocking outgoing longwave radiation and producing precipitation, clouds are a factor of great impact in the Earth's climate. The single major source of uncertainty in global climate models has only been of the clouds responsibility, especially when they are running low. Nowadays it is still a challenge to model the clouds conduct. Therefore, it is of great relevance to monitor changes in Earth's cloud cover and movements [49].

Habitually, the clouds behavior has been observed at naked eye by trained technicians at weather stations or at onboard ships around the world, following the rules of the World Meteorological Organization (WMO). Then, the collected data is transmitted through the Global Telecommunication System (GTS) in real time to weather stations all around the world [49].

In what concerns the solar forecasting, one of the most important factors of photovoltaic systems is the predictability of solar radiation, which is greatly dependent on cloudiness, which occurrence is a non-linear process [50]. This doesn't mean that when a cloudy day happens, the PV system stops functioning, it stills produces power, although not in the quantity it would in a clear sky day. This is called low-light condition performance.

2.2.5. *Solar Altitude*

Solar altitude refers to the angular height of the sun in the sky measured from the horizon. The elevation is 0º at sunrise and 90º when the sun is directly overhead, which may never truly happen, depending on the location's latitude. The elevation angle varies during the day, and is also dependent of the latitude of the location and of the time of the year. An important parameter in the design of photovoltaic systems is the maximum elevation angle, that is, the maximum height of the sun in the sky at a particular time of year. This is important for photovoltaic systems, because it can affect the intensity of the energy that reaches solar panels [51].

While the maximum elevation angle is used even in very simple PV systems design, more precise PV systems require the exact variation of the maximum angle throughout the day. The elevation angle can be calculated using the following equation:

$$\alpha = \sin^{-1}[\sin\delta \,.\, \sin\varphi + \cos\delta \cos\varphi \cos(HRA)]$$

Where,

α is the elevation angle;

δ is the declination angle;

φ is the latitude of the current location;

HRA is the hour angle.

The zenith angle is the angle between the sun and the vertical. The zenith angle is similar to the elevation angle but it is measured from the vertical rather than the horizontal, thus making the zenith angle (ζ) = 90° - elevation [51]. This can be seen next in Figure 2.6.

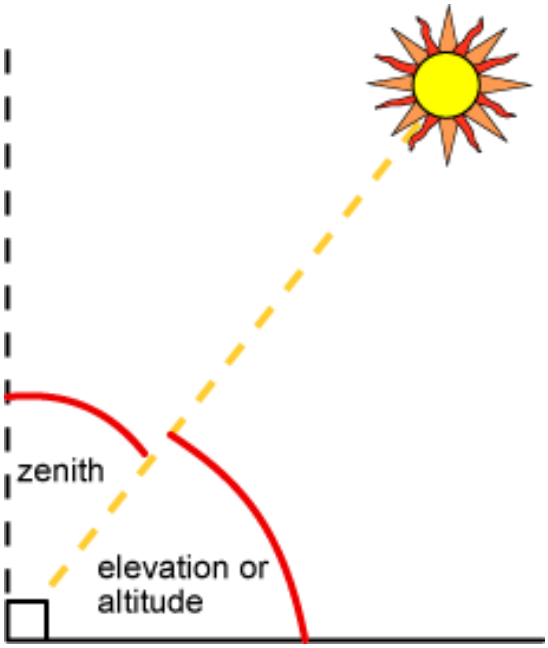

Figure 2.6 – Zenith angle [51]

Chapter 3

State of the Art

The power output of a photovoltaic system is very dependent of the weather conditions, especially the global horizontal irradiance. As the irradiance is very unstable, varying not only seasonally but also daily, it comes out as a challenging forecasting object. The importance of photovoltaic power output forecasting is therefore of great relevance. This chapter presents a review over some photovoltaic power forecasting models and does a review over the state of the art of such models.

With the study of the state of the art will be possible to better understand the relevance of the present thesis and its innovations.

3.1. Solar Forecasting Models

Solar radiation is the driving force behind a number of solar energy devices with a great range of action and operating principles such as the aforementioned photovoltaic systems which generate energy, solar collectors for building heating, air conditioning climate control in buildings and some passive solar devices such as windows, walls or even floors [19].

As stated before, the introduction of renewable energy in the markets has been gradually rising, but it still is a big controversy source. It has undoubtedly a great potential in terms of economic and environmental causes, but its instability and great volatility, are the big challenge to be surpassed.

Along the years some methods targeting the solution to this problem have been developed. The forecasting horizon is a very import factor, since some methods are better for a particular horizon than others. Therefore, this chapter describes some of these methods.

Also, a necessary remark concerning this state of the art section is the difficulty in finding previous work in the particularity of this thesis which is hybrid models between Autoregressive and Numerical Weather Prediction models. Photovoltaic power production is notoriously rising throughout the world and when the PV forecasting existing studies is compared to the corresponding offer for wind farm power production forecasting it stands out the gap between both technologies, with prejudice to the PV power production forecasting.

3.1.1. *Physical Models*

3.1.1.1. Solar irradiance forecast using satellite images

As far as short-term horizons are concerned, satellite data are a high quality source for radiance information because of its excellent temporal and spatial resolution. Due to the strong impact of cloudiness on surface solar irradiance, an accurate description of the temporal development of the cloud situation is essential for irradiance forecasting. As a measure of cloudiness, cloud index images according to the Heliosat method [35], a semi-empirical method to derive solar irradiance from satellite data, are calculated from the satellite data. To predict the cloud index image in a first step motion vector fields are derived from two consecutive images. The future image then is determined by applying the calculated motion vector field to the actual image. At last, solar surface irradiance is derived from the predicted cloud index images with the aid of the Heliosat method [21].

As a measure of cloudiness a dimensionless cloud index value n for each image pixel is derived. A basically linear relationship is assumed to describe the influence of the cloud index on the atmospheric transmittance. The global irradiance is calculated by combining the information on the atmospheric transmission with a clear sky model.

Typical deviations of hourly satellite-derived global irradiance from ground truth data are 20-25% of relative root mean square error (RMSE) for Meteosat7. For the new satellite generation Meteosat second generation (MSG) and using further enhanced irradiance calculation schemes these errors are reduced with a factor of approx. 0.9. The quality of the satellite-derived irradiance provides a lower limit for the forecast accuracy [23].

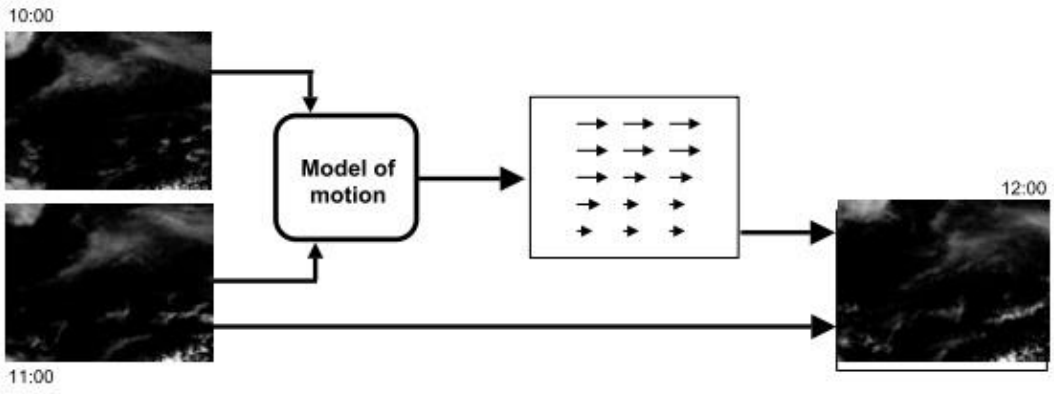

Figure 3.1 - Motion vector fields calculated in short-term forecasting scheme [21]

3.1.1.2. Numerical Weather predictions

Very short-term forecasting of global solar irradiance with a limited time horizon of approximately 6h is not sufficient for an efficient planning and operation of solar energy systems. Especially for the grid integration of solar energy forecasts for up to 48h or even beyond have to be provided. Numerical meteorological models may have the potential to satisfy the requirements in forecasting solar irradiance. A meteorological model is any model which allows calculating fields of meteorological variables, e.g., wind speed, radiation in the atmosphere. Global NWP models have usually a coarse resolution and do not allow for a detailed mapping of small-scale features. Therefore, the use of regional mesoscale models and the combination of a NWP model with a statistical post-processing tools to account for local effects needs to be evaluated and are presented here [23].

The development of NWP tools have been helping in the constant advance of power forecasting technologies for electric power plants based on renewable energies. These tools have the objective, from given initial conditions, to supply information for a specific area, concerning atmospheric conditions for a specified time horizon [66].

Forecasts beyond 6h, up to several days ahead, are usually most accurate when derived from NWP models. These models predict GHI using columnar (1D) radiative transfer models. Heineman et al. [21] showed that the MM5 mesoscale can predict GHI in clear skies without mean bias error (MBE). However, the bias was highly correlated with cloudiness and becomes strong in overcast conditions [67].

The numerical weather predictions can be divided in two different categories, global, which provide forecasts all around the world and local, which provide forecasting for determined regions.

The global models provide meteorological forecasts in a large scale, mostly for each hemisphere. These models usually have a resolution of 200km and its main goal is identifying the global atmosphere behavior of determined zone. Once the NWP are complex

mathematical models, they are usually performed by clusters of computers, which can limit its usability for short-term forecasts due to the computational power and time it requires. For this reason they are mostly used in forecasting horizons superior to 6 hours [24].

The local models focus mostly on big areas (usually countries), and have a spatial resolution from 2km to 50km. Their objective is to identify and analyze in great detail the atmospheric behavior above a specific region, recognizing, therefore, small scale meteorological phenomenon. These models are of extreme importance for solar and wind power plants, since they allow a great resolution study of a specific geographical zone. However, higher resolution requires higher processing power which raises the processing time [24].

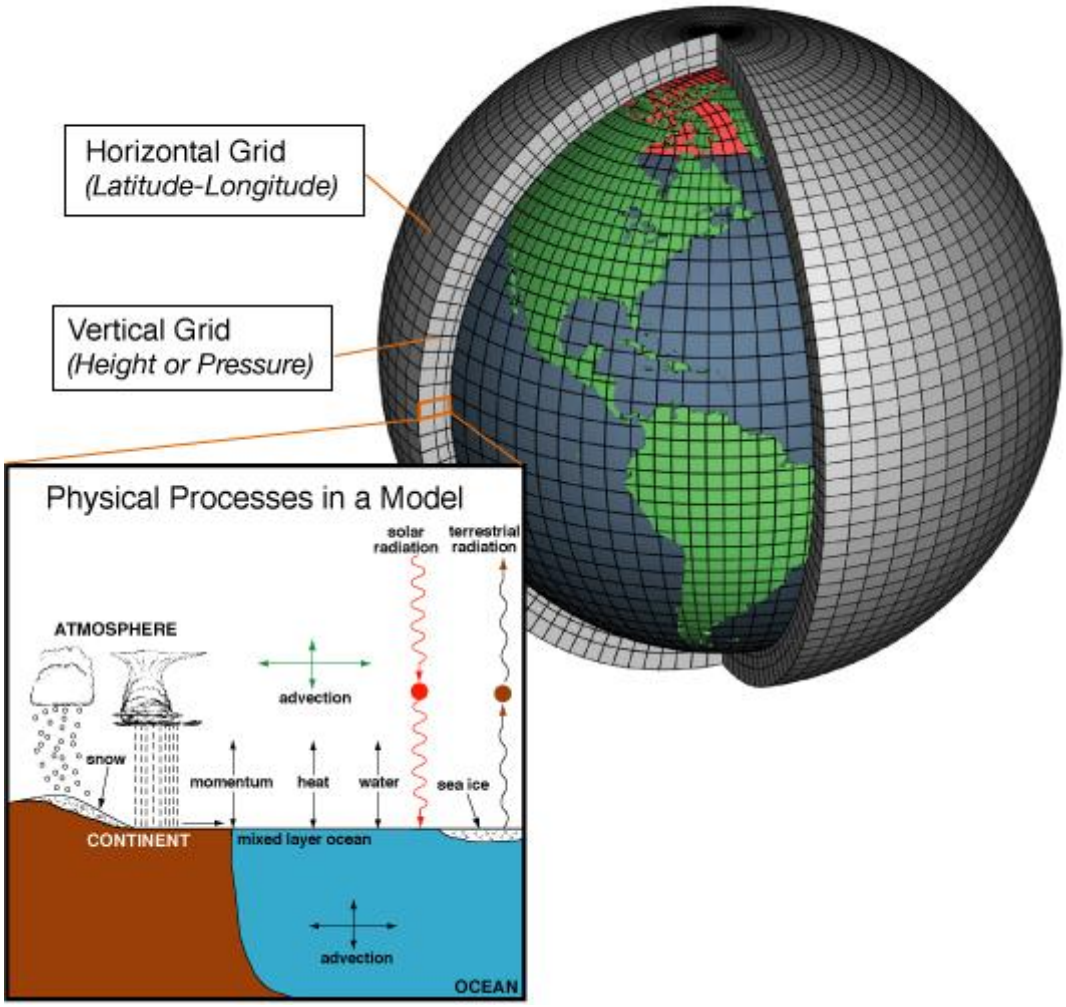

Figure 3.2 – An example of the planet divided into a 3-D grid for the purpose of NWP [30]

Mathiesen and Kleissl [65] found that it was of interest to compare bias-corrected NWP model forecasts to other more advanced models by specialized renewable energies forecasts providers. As the accuracy of bias-corrected NWP forecasts provide a useful reference to other models. Also, the NWP models were shown to be significantly biased towards forecasting clear skies.

Lorenz et al. [70] presented an approach to predict regional PV power output for up to 72 hours ahead using NWP provided by the European Centre for Medium-Range Weather Forecasts (ECMRWF). This work was specially focused on the solar irradiance forecasting, which is the most relevant variable for PV power prediction. An optimum adjustment of the temporal resolution was achieved by combining their model with a clear sky model to regard the typical diurnal irradiance course. In this work they proposed and evaluated an approach to derive weather specific prediction intervals. The derived prediction intervals provide a reasonable estimate for the expected maximum deviation of the measures from the predicted values. It was also found that the accuracy of the global horizontal irradiance forecast is the decisive factor for the accuracy of the PV power forecast.

Remund et al. [76] compared and evaluated several different NWP models in order to forecast Global Horizontal Radiation (GHI), all used in the USA but in three different locations and climates. The authors reported relative RMSE ranging from above 20% to almost 50% and the breakeven of persistence is reached after 2-4 hours.

Perez et al. [77] studied and validated the short and medium term global irradiance forecasts that are produced as part of the US Solar Anywhere data set. The short term forecasts that extend up to 6 hours ahead are based upon cloud motion which is derived from geostationary satellite images. While the medium term forecasts extend up to 6 days ahead and are modeled from gridded cloud cover forecasts. The authors reached a conclusion that the NWP-based forecasts perform significantly better than persistence. Also, they found that the satellite-derived cloud motion-based forecasting lead to a major improvement over NDFD (National Digital Forecast Database) forecasts up to 5 hours ahead. While one hour forecasts are similar or a little better than the satellite model from which they derive.

Lorenz et al. [79] introduced a benchmarking procedure to test the accuracy of irradiance forecasts and to compare different forecasting methods. The conclusion of the evaluation executed by the authors shows a strong dependence of the forecast accuracy on the climatic conditions. Concerning Central European stations the relative RMSE ranges from 40% to 60%. For Spanish stations, relative RMSE ranges from 20% to 35%. The authors found that irradiance forecasts based on global model numerical weather prediction models in combination with post-processing show the best results. Also, all the studied methods reached better results than the persistence.

3.1.2. *Computational Models*

3.1.2.1. ARMA

The ARMA model is usually applied to auto correlated time series data as used by Box and Jenkins [20]. This model is a good tool to understanding and predicting the future value of a specified time series. ARMA is a conjugation of two different parts, the autoregressive (AR) and the moving average (MA). This model is usually referred as ARMA (p,q), where p is the order of AR and the q is the order of MA. AR models are based in the assumption that the current series of values can be explained by its past values. The MA model is an alternative to the AR models, where the current value of the series can be explained by the pondered sum of previous terms on the noises or residuals. So, ARMA (1,1) is the simplest form that this method can achieve [22].

In 1987, Chowdhury and Rahman, used sub-hourly data to forecast solar radiation. It was used for the first time an initial cleaning process where the transmissivity between clear sky days and cloudy days are separated. For clear sky days, the authors considered the existing physical equations were sufficient when joined by the parametrical values for the study area. For the transmissivity on cloudy days an ARMA model was used [63].

In different studies, Hokoi et al. [64], developed a time series stochastic model of hourly solar radiation for the summer months. In this work the ARMA (3,3) model provided better results. The auto-correlation function between the actual data and the simulated data were coincident for small spans of time. However, for larger spans of time the simulated data does not follow the fluctuations of the actual data, although they lean for the same mean value.

Wu and Chang [22], applied a classical ARMA model to a stationary solar radiation series, while checking its order according to auto correlation and partial correlation, and concluded that the best order is ARMA (1,1). Although the ARMA model is very stable, the authors completed their method with a TDNN (Time Delay Neural Network) model which is more sensitive to make the best of both models and reach a forecast of hourly solar radiation.

3.1.2.2. ARIMA

The ARIMA models are non stationary time series, which were also considered earlier by Yaglom [20], are of fundamental importance to problems of forecasting and control. A stationary time series is one whose average and standard deviation are stable throughout the series. So time series with trends, or with seasonality, are non-stationary. i.e., the trend and seasonality will affect the value of the time series at different times. On the other hand, a white noise series is stationary, it does not matter when it is observed, it should look the same at any period of time. When a look is taken at Figure 3.3 it can be noticed that the Dow

Jones index data was non-stationary in (a), but the daily changes were stationary in (b). This shows one way to make a time series stationary, i.e., compute differences between consecutive observations. This is known as differencing.

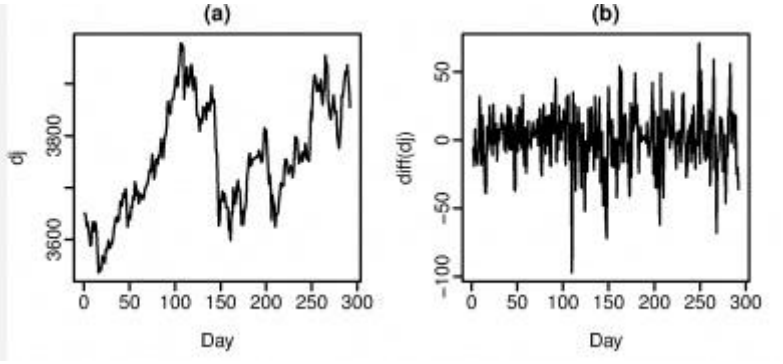

Figure 3.3 - a) Dow Jones index on 292 consecutive days; b) Daily change in Dow Jones 292 consecutive days [18]

If differencing and autoregression are combined with a moving average model, a non-seasonal ARIMA model is obtained. The full model can be written as

$$y'_t = c + \varphi_1 y'_{t-1} + \ldots + \varphi_p y'_{t-p} + \theta_q e_{t-1} + \ldots + \theta_q e_{t-q} + e_t$$

Where $y'_t$is the differenced series (it may have been differenced more than once). The "predictors" on the right hand side include both lagged values of $y_t$and lagged errors. This is called ARIMA (p,d,q) model. Once the combination of components in this way to form more complicated models, it is much easier to work with the backshift notation [18]. The biggest advantage of the ARIMA method in forecasting is that the extrapolations do not accumulate errors from other variables throughout the process.

Reikard [74] applies a regression in log to the inputs of the ARIMA models to predict the solar radiation. ARIMA models are compared with other forecast methods such as ANN. At the 24 hour horizon, Reikard states that the ARIMA model captures the sharp transitions in irradiance associated with the diurnal cycle more accurately than other methods.

Hamilton [75] states that ARIMA techniques are reference estimators in the prediction of global radiation field. It is a stochastic process coupling autoregressive (AR) component to a moving average (MA) component.

3.1.2.3. Artificial Neural Networks

Artificial neural networks (ANN) have powerful pattern recognition and pattern classification capabilities. Inspired by biological systems particularly by research into human brain, ANN's

are able to learn from and generalize from experience. Currently, ANN's are being used for a wide variety of tasks in many fields of business, industry and science [25].

One major application area of ANN's is forecasting. ANN's provide an attractive alternative tool for both forecasting researchers and practitioners. Several distinguishing features of ANN's make them valuable and attractive for a forecasting task. As opposed to the traditional model-based methods, ANN's are data-driven self-adaptive methods in that there are a few a priori assumptions about the models for problems under study. They learn from examples and capture subtle functional relationships among the data even if the underlying relationships are unknown or hard to describe. Thus ANN's are well suited for problems whose solutions require knowledge that is difficult to specify but for which there are enough data or observations. In this sense they can be treated as one of the multivariate nonlinear nonparametric statistical methods. This modeling approach with the ability to learn from experience is very useful for many practical problems since it is often easier to have data than to have good theoretical guesses about the underlying laws governing the systems from which data are generated [25][52].

Great efforts were made in order to generate solar power forecasting methods using ANNs, since the irradiance fluctuates depending on weather conditions. So the results are significantly dependent on the quality of weather forecasts. In some electric enterprises, irradiance prediction is a very important tool for hybrid power systems with batteries. So ANN provides better forecasts of PV power production, allowing e.g. more profitability [54].

Paoli et al. [68], developed an ANN prediction approach to determine global irradiation at a daily horizon, which can help electrical managers with grid-connected PV power systems, using as ad hoc time series pre-processing based on clear sky indexes. The conclusion was that without time series pre-processing the achieved results are not as good as when the time series are pre-processed.

Mellit and Pavan [69] proposed a practical method for solar irradiance forecasting using ANN. They proposed a Multilayer Perceptron (MLP) model that makes possible the forecasting of solar irradiance for a 24h span, using present values of the mean daily irradiance and air temperature. In this study, it was found that due to the complex architecture of the MLP forecasting method in terms of computing time needed to achieve good performances, ANN trained by genetic algorithms will be used in the future with the objective of reducing the number of iterations and consequently the computing time. Also, they found that to obtain more accurate forecasts a larger database is required (more than a year worth of data).

Sfetsos and Coonick [19] used ANN to make single step predictions of mean hourly values of global irradiance and reached the conclusion that these models have a better performance over linear time series models which are based on the forecasting of clearness indexes.

Cao and Cao [77] developed a hybrid model for forecasting sequences of total daily solar radiation, which combines Artificial Neural Networks with wavelet analysis. The method used in this study was applied to solar irradiance forecasting and presented relevant improvements in the accuracy of the forecast for the day-to-day solar irradiance of a year comparing to when the wavelet analysis was not used.

3.1.2.4. Support vector Machines

A different statistical method is the Support Vector Machines (SVM). Support vector machines are based on the "Structural Risk Minimization" principle from computational learning theory. The idea of structural risk minimization is to find a hypothesis h for which the lowest true error can be guaranteed. The true error of h is the probability that h will make an error on an unseen and randomly selected test sample. An upper bound can be used to connect the true error of a hypothesis h with the error of h on the training set and the complexity of H (measured by VC (Vapnik-Chervonenkis) Dimension), the hypothesis space containing h. Support vector machines find the hypothesis h which (approximately) minimizes the bound on the true error by effectively and efficiently controlling the VC-Dimension of H [33]. The VC dimension of a set of functions is the size of the largest data set due to that the set of functions can scatter [34].

SVM's are very universal learners. In their basic form, SVM's learn linear threshold function. Nevertheless, by a simple "plug-in" of an appropriate kernel function, they can be used to learn polynomial classifiers, radial basic function (RBF) networks, and three-layer sigmoid neural nets [32].

The success of using SVMs for time series prediction is greatly due to its outstanding ability of generalization. In a SVM, the historical data of the time series is mapped into a higher-dimensional feature space by a nonlinear mapping. Then, a linear regression is utilized in the higher-dimensional feature space to elaborate the time series predictions, which is simply an alternative way to solve a nonlinear regression problem. They key to solve this prediction problem is to find optimal values for the weights and biases parameters of the SVM [55].

Zeng and Qiao [55] found that in terms of forecasting accuracy, SVM-based models significantly outperformed autoregressive models, because of its superior ability of learning nonlinear and time-varying nature of solar radiation data. Also, SVM models outperformed BBFNN models, which is mostly due to the good generalization of SVMs. The model developed by Zeng and Qiao used a new 2D representation for hourly solar radiation, which provides a greater capability of understanding the solar radiation pattern when compared to the usal 1D representation.

Support vector regression (SVR) is the most common application form of SVM's. SVR is a technique of nonlinear regression based on SVM's. This technique is commonly used in the

pattern recognition and text classification areas. Instead of minimizing the obtained training error, SVR tries to minimize the frontier of the error, so a generalized performance is achieved. The concept of SVR is based in computational calculations of a linear regression function in a space of big dimensional characteristic, where the input data is mapped through a non linear function. SVR has been applied in a vast selection of fields, e.g., time series forecasting, high complexity approximation of engineering analysis, etc [35].

3.2. Final Remarks

As seen in the previous chapter, Photovoltaic power production forecasting is a very relevant field of study and a deeper knowledge is yet to be reached in this area of work. Especially if one has the notion that solar power is the larger source of energy the humanity has access to.

By analyzing the State of the Art chapter, a conclusion can be drawn that although some studies have been done in the field of photovoltaic power forecasting, not many of them propose a hybrid model between Numerical Weather Predictions and Autoregressive models. This is one of the focuses of the present thesis.

Also, a relatively new statistical method known as Extreme Learning Machines is used. This method is not much well known, yet, as seen above, particularly concerning solar power forecasting, which is almost non-existing.

This thesis' main objective is to apply Extreme Learning Machines to photovoltaic power production forecasting, trying, thus, to take a step further and fill the gap found in this field of work.

Chapter 4

Methodology

The proposed method for this thesis is a hybrid model between Extreme Learning Machines (ELM) and an autoregressive method, for short-term forecasting, i.e., for up until 72 hours ahead, using Numerical Weather Predictions (NWP) as well as series of past values.

This chapter gives an overview about Extreme Learning Machines and makes a few comparisons with other statistical methods commonly used for forecasting, and which were also used in this work in terms of checking and validation of the obtained results.

Also, this chapter covers the data treatment process for the variables of the proposed problem. And does an overview of the forecasting model layout used in this thesis. In the end, this chapter presents the activation functions utilized in this work.

4.1. Artificial Neural Networks

Artificial Neural Networks (ANN) can generalize, i.e., after learning the data presented to them, which is called a sample, ANN's can often correctly deduce the unseen part of a population even if the sample data contain noisy information. As forecasting is performed via prediction of future behavior (the unseen part) from examples of past behavior, it is an ideal application area for neural networks, at least in principle. Any forecasting model assumes that there exists an underlying (known or unknown) relationship between the inputs, which can be past values or any other relevant variables, and the outputs. Frequently, traditional statistical forecasting models have limitations in estimating this underlying function due to the complexity of the real system [25].

Also, ANN's are nonlinear, while most traditional methods such as the Box-Jenkins or other ARIMA method, assume that the time series under study are generated from linear processes.

However, ARIMA-like methods may be totally inappropriate if the underlying mechanism is nonlinear. It is unreasonable to assume a priori that a particular realization of a given time series is generated by a linear process. In fact, real world systems are often nonlinear [25].

An ANN can be created by simulating a network of model neurons in a computer. By applying algorithms that mimic the process of real neurons, we can make the network “learn” to solve many types of problems. A model neuron is referred to as a threshold unit and its function can be viewed in Figure 4.1 [26].

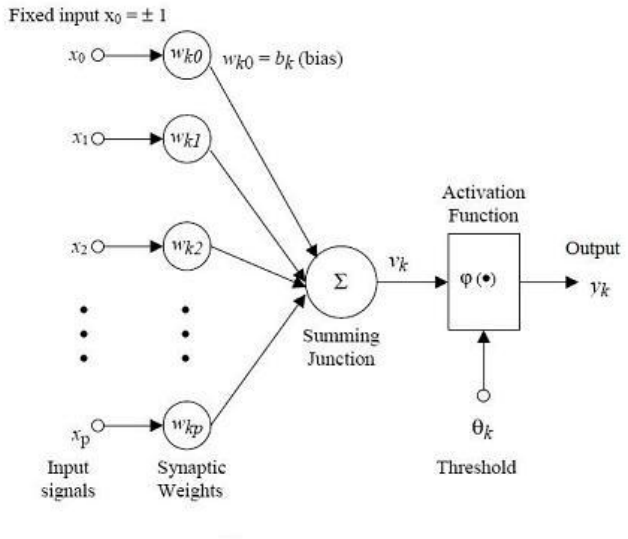

Figure 4.1 - Schematization of an artificial neural networks's neuron model [27]

It receives input from a number of other units or external sources, weighs each input and adds them up. The total input is then passed by an activation function, which can be of various different types. If the total input is above a threshold, the output of the unit is one; otherwise it is zero. Therefore the output changes from zero to one when the total weighted sum of inputs is equal to the threshold. The points in input space satisfying this condition define a so called hyperplane. In two dimensions, a hyperplane is a line, whereas in three dimensions, it is a normal plane [26].

The standard way of an ANN is to group the neurons into N layers, including one input layer, and up to several hidden or internal layers. Such a network is illustrated in Figure 4.2. Notice that in a network, a given neuron isn’t necessarily connected to all neurons in the next. This is what is called a sparse network. A complete ANN is one in which any given neuron is connected to every neuron in the next layer [28].

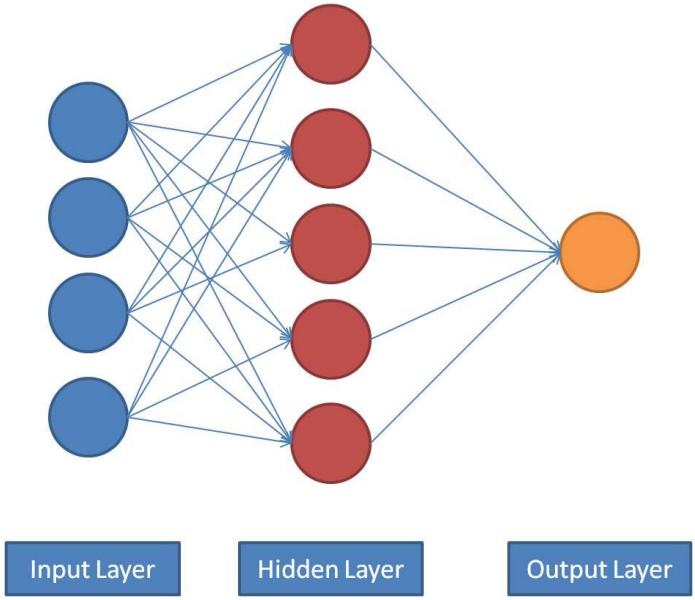

Figure 4.2 - Example of an artificial neural network with layers

The input layer can be thought as the "sensor organ" of the ANN. It is where the parameters of the environment are set (i.e. the information the ANN is required to make a decision about). The neurons in this layer have no incoming connections, since their values are set from an external source. The outgoing connections send these values to the neurons of the next layer in the forward direction [28].

In between the input and output layers, a series of one or more "hidden" layers are set. The reason they are called hidden is that they are invisible to any external processes that interact with the ANN. The neurons in these layers have both incoming connections from the preceding layers as well as outgoing connections to the succeeding layer, and work as described previously in this section. The hidden layers can be thought of as the "cognitive brain" of the network [28].

The output layer holds the end of the parameters of a problem, the information here can be interpreted as the proposed solution. The neurons in this layer have no outgoing connections, because their values are read directly by whatever external process is using the network [28].

To test the neural network, the problem information is simply loaded into the input layer neurons, and is computed for every neuron in each of the succeeding layers (layer by layer until the output layer is reached). The resulting values in the output layer will greatly depend on what training the network has been previously exposed to [28].

4.2. Support Vector Machines

Support Vector machines (SVMs) and its variants, have been widely used in the past in classifications and regression problems. SVM has two main learning features [37]:

- In SVM, the training data are first mapped into a higher dimensional feature space through a nonlinear feature mapping function $\varphi(x)$
- The standard optimization method is then used to find the solution of maximizing the separating margin of two different classes in this feature space while minimizing the training errors.

With the introduction of the epsilon-insensitive loss function, the support vector method has been extended to solve regression problems [37].

As the training of SVMs involves a quadratic programming problem, the computational complexity of SVM training algorithms is usually intensive, which is at least quadratic with respect to the number of training examples. It is difficult to deal with large problems using single traditional SVMs, instead SVM mixtures can be used in large applications. SVM mixtures allow the use of different experts in different regions of the input space and also support easy combinations of several architectures such as polynomial networks and radial basis function networks [72]. Least square SVM (LS-SVM) and proximal SVM (PSVM) provide fast implementations of the traditional SVM [37].

4.3. Extreme Learning Machines

Recently a learning algorithm called Extreme Learning Machine (ELM) has been proposed for single-hidden layer feedforward neural networks (SLFN) with additive neurons to easily achieve good generalization performance at extremely fast learning speed [36].

This section is dedicated to Extreme Learning Machines, first an introduction is made, then, this method is compared to other statistical methods.

4.3.1. *ELM Basics*

Extreme Learning Machines (ELM) were originally proposed for the single-hidden-layer feedforward network and were then generalized SLFNs where the hidden layer needs not to

be neuron alike [37]. ELM randomly chooses the input weights of SLFN, then the output weights (linking the hidden layer to the output layer) of an SLFN is analytically determined by the minimum norm least-squares solutions of a general system of linear equations. The running speed of ELM can be thousands of times faster than traditional iterative implementations of SLFNs [38].

More specifically, the output function of ELM for generalized SLFNs, as an example, is

$$f_L(x) = \sum_{i=1}^{L} \beta_i h_i(x) = h(x)\beta$$

Where $\beta = [\beta_1, \dots, \beta_L]^T$ is the vector of the output weights between the hidden layer of L nodes and the output node and $h(x) = [h_1(x), \dots, h_L(x)]^T$ is the output vector of the hidden layer with respect to the input x. h(x) actually maps the data from the d-dimensional input space (ELM feature space) H, and thus, h(x) is indeed a feature mapping, this is illustrated by Figure 4.3. For the binary classification applications, the decision function ELM is

$$f_L(x) = sign(h(x)\beta)$$

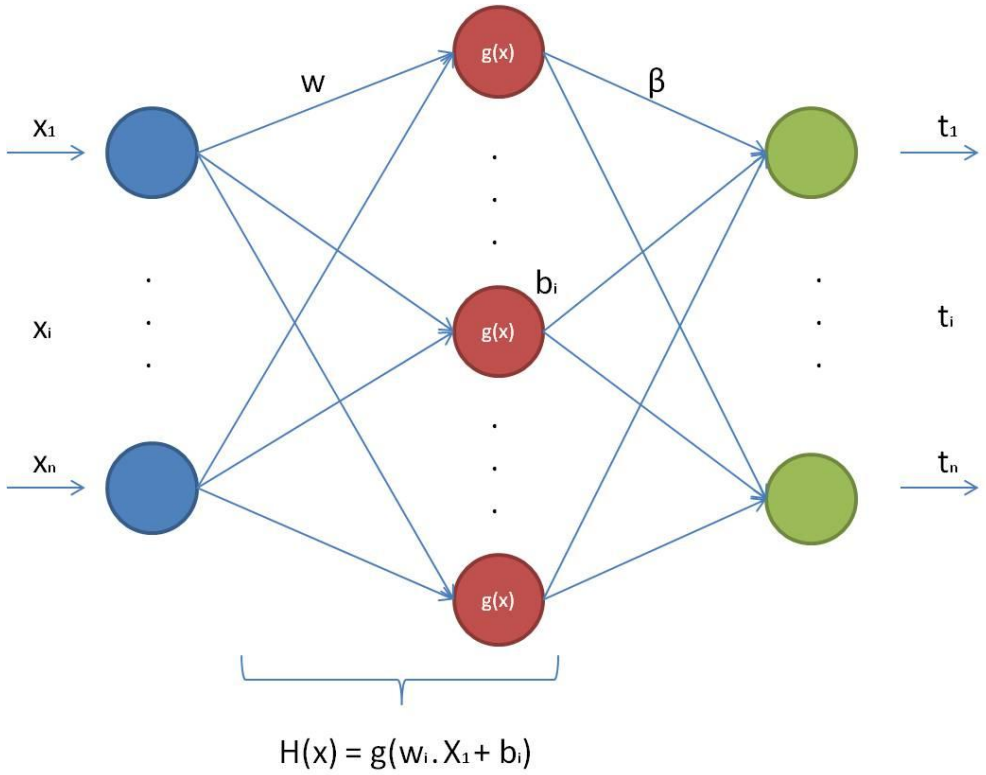

Figure 4.3 - Structure of an ELM network

Different from traditional learning algorithms, ELM tends to reach not only the smallest training error but also the smallest norm of output weights. According to Bartlett's theory

[43], for feedforward neural networks reaching smaller training error, the smaller the norms of weights are, the better generalization performance the networks tend to have. ELM is to minimize the training error as well as the norm of the output weights

$$min: \|H\beta - T\|^2 \; and \; \|\beta\|$$

Where H is the hidden-layer output matrix

$$H = \begin{bmatrix} h(x_1) \\ \vdots \\ h(x_N) \end{bmatrix} = \begin{bmatrix} h_1(x_1) & \dots & h_L(x_1) \\ \vdots & \vdots & \vdots \\ h_1(x_N) & \dots & h_L(x_N) \end{bmatrix}$$

According to Liu, He and Shi [38], to minimize the norm of the output weights $\|\beta\|$ is actually to maximize the distance of the separating margins of the two different classes in ELM feature space [37].

The minimal norm least square method instead of the standard optimization method was used in the original implementation of ELM

$$\beta = H^{\dagger} T$$

Where $H^{\dagger}$ is the Moore-Penrose generalized inverse of matrix H, which is presented in Appendix B. Different methods can be used to calculate de Moore-Penrose generalized inverse of a matrix: Orthogonal projection method, orthogonalization method, iterative method and single value decomposition (SVD) [37].

The ELM is based on two theorems [39]:

Theorem 1: *Given a standard SLFN with N hidden nodes and activation function* $g : R \to R$ *which is infinitely differentiable in any interval, for N arbitrary distinct samples* (x_i, x_t)*, where* $x_i \in R^n$ *and* $t_i \in R^m$*, for any* w_i *and* b_i *randomly chosen from any intervals of* R^n *and R, respectively, according to any continuous probability distribution, then with probability one, the hidden layer output matrix H of SLFN is invertible and* $\|H\beta - T\| = 0$ *[39].*

Theorem 2: *Given any small positive value* $\varepsilon > 0$ *and activation function* $g : R \to R$ *which is infinitely differentiable in any interval, there exists* $\widetilde{N} \leq N$ *such that for N arbitrary distinct samples* x_i, x_t *where* $x_i \in R^n$ *and* $t_i \in R^m$*, for any* w_i *and* b_i*randomly chosen from any intervals of* R^n *and R, respectively, according to any continuous probability distribution, then with probability one* $\|H_{NxN}\beta_{Nxm} - T_{Nxm}\| < \varepsilon$ *[39].*

These theorems show that it is possible to randomly choose N bias values for N hidden nodes such that the corresponding vectors span $\mathrm{R^N}$. This means that for any weight vectors and bias values chosen from any intervals of $\mathrm{R^N}$or R, respectively, according to any continuous probability distribution, then the column vectors of H can be made full-rank.

Both these theorems are proved and further discussed by Huang et al. in [39].

4.3.2. *ELM vs. Neural Networks*

In terms of comparison between artificial neural networks and extreme learning machines, the first thing that comes up is that ANN can be used for feedforward neural networks with more than one hidden layer, while the ELM only uses one hidden layer as it is. Luckily, SLFN can be used to approximate any continuous function [56]. Also, in the ELM case, the input layer is randomly generated, while the ANN has its input layer analytically calculated.

Another truly important characteristic of the ANN is that they are trained with back-propagation or other iterative algorithms, while the ELM is not. A great advantage of the ELM in relation to ANN is its learning speed which is extremely fast. ELM can train SLFN much faster than the traditional ANN, as before there seemed to be a speed barrier which most classic learning algorithms seemed incapable of surpassing, as it wasn't unusual to take a very long time to train a network using ANN [56].

Also, ELM tends to reach the smallest training error, as well as the smallest norm of weights. Therefore, it tends to reach a better generalization for the proposed problems [56].

Finally, a note for the remarkable simplicity of ELMs compared to ANNs.

4.3.3. *ELM vs. SVMs*

Latest development of ELM has shown some relationships between ELM e SVM [38]. Suykens and Vandewalle[41] described a training method for SLFNs which applies the hidden-layer output mapping as the feature mapping of SVM. However, the hidden-layer parameters need to be iteratively computed by solving an optimization problem. The authors of this method identified some drawbacks, which are the high computational cost and larger number of parameters in the hidden layer. Other studies, such as [38] and [40] show that the ELM learning approach can be applied to SVMs directly by simply replacing SVM kernels with random ELM kernels and better generalization can be achieved. Instead of using a parametric hidden layer as done in [42], these studies use a nonparametric hidden-layer in the ELM, and the hidden-layer parameters need not be tuned and can be fixed once randomly generated [37].

Huang et al. [42] achieved the following conclusions:

1) SVM's maximal separating margin property and the ELM's minimal norm of output weight property are actually consistent, and with ELM framework, SVM's maximal separating margin property and Barttlet's [43] theory on feedforward neural networks remain consistent.

2) Compared to SVM, ELM requires fewer optimizations constraints and results in simpler implementation, faster learning and better generalization performance.

However, similar to SVM, inequality optimization constraints are used by Huang et al. [42], as well as random kernels and the term bias b used in the conventional SVM is discarded. Nonetheless, no direct relationship has been found between the original ELM implementation and the mixtures of the original SVM method, like LS-SVM and PSVM [37].

According to Huang et al. [37] ELM, which is with higher scalability and less computational complexity, not only unifies different popular learning algorithms but also provides a unified solution to different practical applications. Different variants of LS-SVM and SVM are required for different types of applications. ELM avoids such trivial and tedious situations faced by the aforementioned methods, since all these applications can be resolved in one formula. Also, from the optimization method point of view, ELM and LS-SVM have the same optimization cost function; However, ELM has milder optimization constraints compared to LS-SVM and PSVM. When compared to ELM, LS-SVM achieves suboptimal solutions and has higher computational complexity; also, the ELM method can run much faster than LS-SVM. ELM with random hidden nodes can run up to tens of thousands times faster than LS-SVM and SVM.

4.4. Data Treatment

The approach which will be taken to the present problem proposes a hybrid model between NWP and past values, with the use of Extreme Learning Machines.

This section presents the steps taken in order to obtain the input variables for the forecasting model.

4.4.1. *Data Organization and Synchronization*

The first step for the data treatment is the synchronization of the data, since both the Numerical Weather Predictions and the Power production of the power plant were in different files, with different organizations.

Once the first step is completed, it will be necessary to elaborate a way to synchronize the past values with the ones previously obtained. The series of past values are

$$P_{t_{-1}}$$

and

$$P_{dayb} = P_{t+K-24\times D}$$

Where $P_{t_{-1}}$ is the power produced one hour before the forecast is made and P_{dayb} is the power produced 24 hours before the hour for which the forecast is being made. t is the hour when the forecast is made, K is the hour of the day for which the forecast will be made. Because the forecasts are made for 72 hours ahead, when the forecast for the 24th hour is being made the power production for 24 hours before is not yet available. Therefore, in order to avoid using forecasts to make forecasts, which would increase the forecasting error, the power production utilized is for 48 hours before, i.e., t_{-48}. The inclusion of the variable D is made for this purpose, {D = 1, 2, 3} and {K=1, …, 72}. Because of this nuance, the first three days of January will need to be eliminated once the series of past values are non-existent.

To give a practical example, a forecast is being made in January's 10th at the hour 9 for the next 3 days/72 hours. For the forecast of the hour 10 of January's 10th, P_{dayb} gets the value of the power produced at the hour 10 of January's 9th, i.e. 24 hours before. When the forecast for the hour 10 of January's 11th is being made, P_{dayb}would ideally get the value of the produced power exactly 24 hours before, i.e. January's 10th, but since that data is not yet available, only a forecasted value is, the value given to that variable is of the hour 10 of January's 9th, i.e., 48 hours before.

The variable $P_{t_{-1}}$is only used through the first 5 hours of the forecast, e.g. if the forecast is made at hour 9 of a certain day, this variable will only affect hours 10 through 14, once as the time goes further, that variable loses interest and importance for the forecasting.

4.4.2. *Clear Sky Model*

At this point, normalization by a clear sky model will be done. As done by Bacher (2008) [1], an estimation of the clear sky model for the solar power will be utilized next, which is explained with more detail in Appendix A. The normalization of the solar power follows the next equation:

$$\tau_t = \frac{P_t}{P_t^{CS}}$$

Where P_t is the solar power obtained from the data files, P_t^{CS} is the clear sky model value for the same *t {t=1,…,26280 }. When* P_t^{CS} *has small values or at nighttime, the values of* τ_t *are tending to infinite. Consequently, the values of the* P_t^{CS} *series where:*

$$\frac{P_t^{CS}}{\max\,[P_t^{CS}\,]} < 0.2$$

Are eliminated from the vector $[\tau_t]$. $\max[P_t^{CS}]$ signifies the maximum value of the P_t^{CS} vector. Other values for the elimination limit were experimented in this process but 0.2 was found to be the most efficient.

4.4.3. *Standardization*

All the data is standardized once every variable has its own scale, and it is advisable to have all data in-between a predetermined set of values, which is [-1, 1]. The used method for this purpose is the min-max, since it is a very simple method and works perfectly well for this purpose. The following equation is used:

$$x' = \frac{x - min_a}{max_a - min_a} \times (max_A - min_A) - min_A$$

Where x' is the standardized value, max_a and min_a are the maximum and minimum values of the series x, respectively, and max_A and min_A are the limit values for the standardized vector, in this case 1 and -1, respectively.

After the forecasts are done, in order to obtain the results in the desired scale, i.e., the original scale, it is necessary to reverse the previous process. So, a procedure called destandardization is performed, in order to return the variables to their original values. This procedure is carried with the following equation:

$$x = \frac{x' - min_A}{max_A - min_A} \times (max_a - min_a) + min_a$$

4.4.4. *Training and Testing Sets*

One important detail about statistical methods such as Extreme Learning Machines is the training and testing sets of data. It is very important that the training set is substantially larger than the testing set. With this in mind, and a with attention that the data set comes down to just one year of data, which is not very large, the sets are divided in a proportion of 2:1.

Since the data set only covers the span of a year, a decision is made of not choosing the testing set following a temporal sequence, e.g., September through December, but to intercalate the testing months between the training months. With this a set of data which covers the entire year is achieved.

4.5. Forecasting Model Layout

The structure of the forecasting model is presented in this section by the following diagrams, the first (Figure 4.4) is an overview of the whole process, the second (Figure 4.5) is a specification of the training and testing structure:

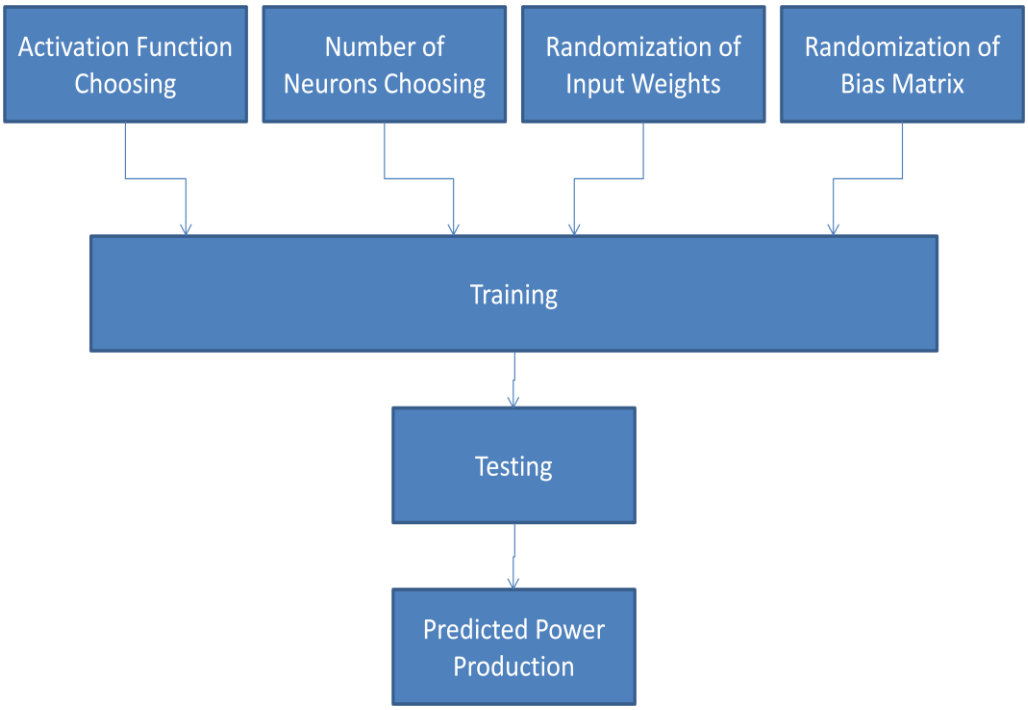

Figure 4.4 – Diagram representing the forecasting model overview

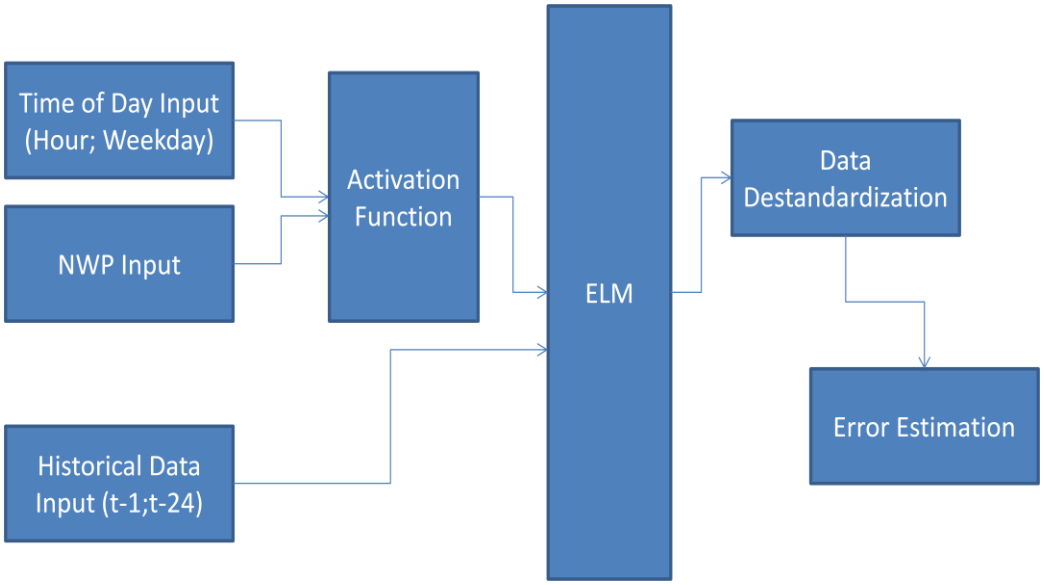

Figure 4.5 - Diagram representing the training and testing structure

The final structure of both training and testing is exactly the same, being the only difference the data sets used for each of the cases.

A network was trained and tested for each of the hours of the time span, i.e., for 72 hours 72 different networks were trained and tested at the same time, and each network had its own different inputs. The networks were tested with different numbers of neurons in order to find the best fit, and several activation functions were also tested. The input weights and biases were randomly generated for every set of networks. Figure 4.6 shows a simplified scheme below:

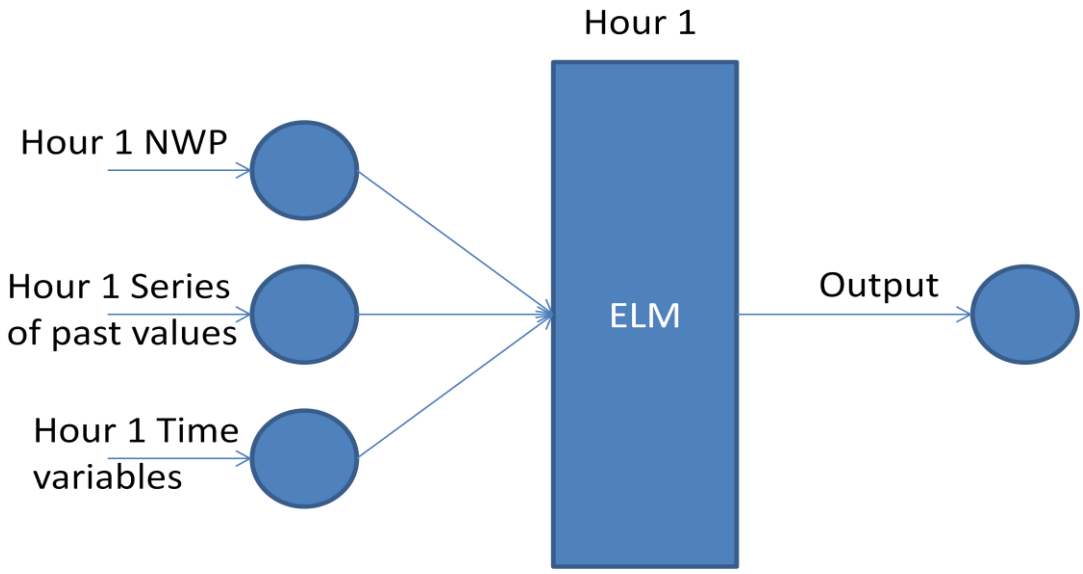

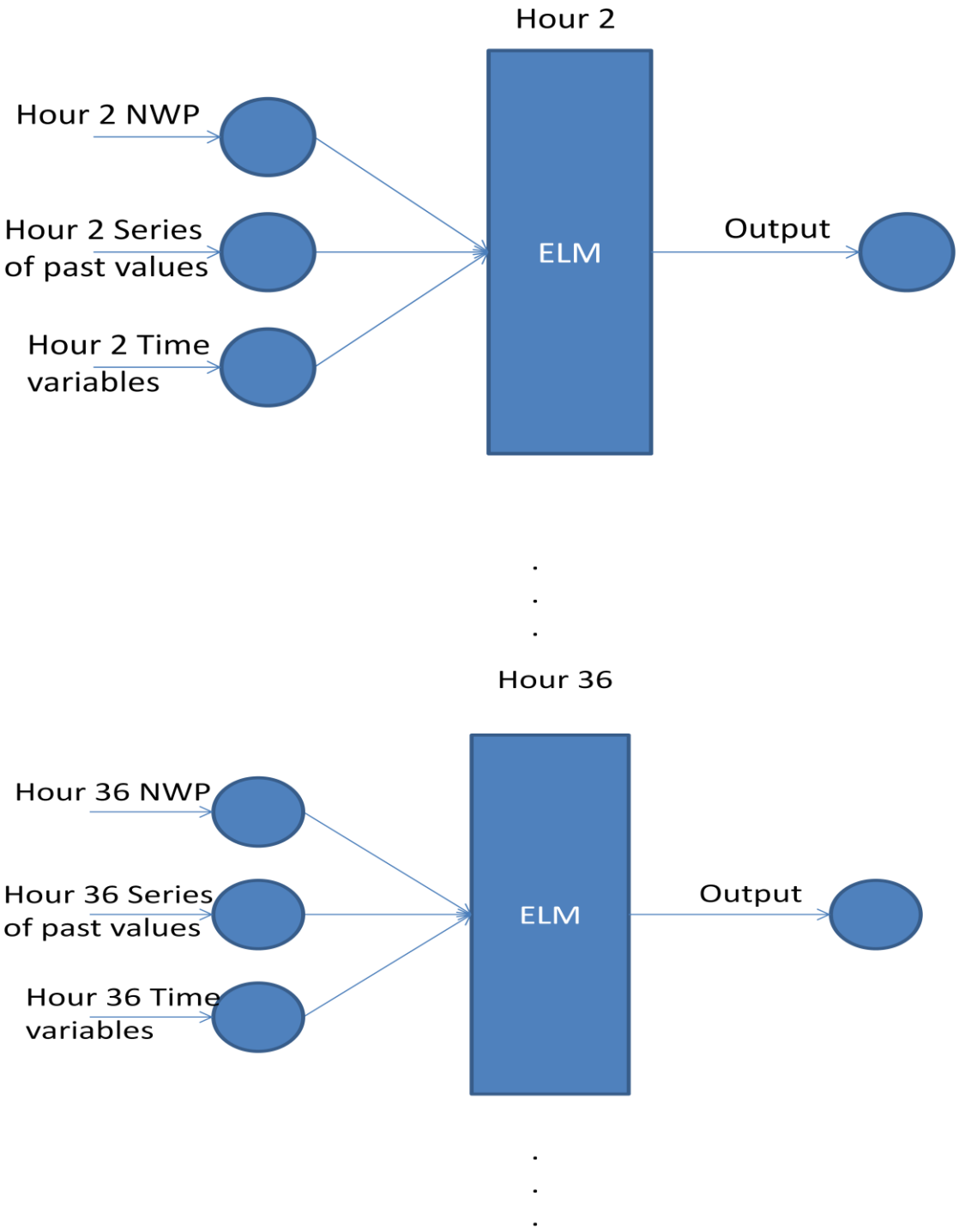
Hour 2
Hour 2 NWP
Hour 2 Series of past values
Hour 2 Time variables
ELM
Output
Hour 36
Hour 36 NWP
Hour 36 Series of past values
Hour 36 Time variables
ELM
Output

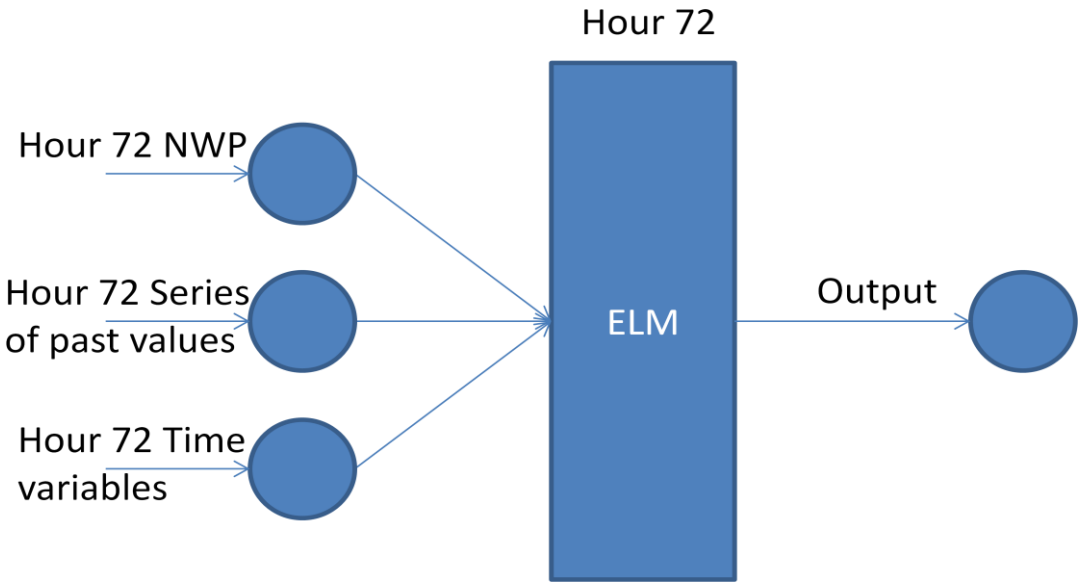

Figure 4.6 - Simplified scheme of the forecasting model for every hour oh the time span

Also, in addition to the ELM, classical neural networks and SVMs were trained and tested with the same inputs for comparison endings.

4.6. Activation Functions

In a neural network, or in this case, an ELM, every neuron has an activation function which stipulates the output of that neuron to an assigned input [58].

In this work, several different activation functions for the hidden layer of the ELM are tested with the purpose of reaching a conclusion of which function provides the best results.

The most commonly used activation function is the logistic function, usually known as the sigmoid function (even tough, the logistic function is just a special case of a sigmoid function), which follows the equation:

$$f(x) = \frac{1}{1 + e^{-x}}$$

Another very commonly used activation function is the sine function. When a sine function is utilized instead of a sigmoid, the learning process seemingly performs decomposition where it

discovers the most important frequency components of the function described by discrete set of input/output examples [59].

$$f(x) = \sin(x)$$

One more activation function utilized in this work is the Radial Basis Function (RBF), which is based on the Gaussian curve. It takes a parameter which determines the mean value of the function used as a desired value. This function is a real-valued one, whose value depends only on the distance to the origin [60]:

$$f(x) = f(\|x\|)$$

Or, alternatively, on the distance to the center point:

$$f(x, c) = f(\|x - c\|)$$

A different transfer function utilized, as well, in the course of this work, was the Hard Limit Function. This function forces a neuron to output a 1 if its net input reaches a threshold, otherwise, it outputs a 0. This allows the neuron to make a decision or classification.

The last activation Function used is the Triangular Basis Function (TBF), which is widely used in different types of neural networks. The TBF is a piece-wise linear (PWL) function. Most neural networks applications utilize symmetrical TBF functions. This makes their design simpler as there is no need to program slopes independently for the transfer function [61].

The aforementioned functions are the ones tested and studied as activation functions in the present thesis. Further details concerning obtained results and comparisons between the functions are approached in the next chapter.

Chapter 5

Results and Discussion

The Photovoltaic power plant used in this case study is located in southern Europe, having, therefore, a similar latitude and climate to the Portuguese case. It is constituted by several PV modules, for study purposes making up to 5 kW of installed power.

The main idea is to make a forecast for each of the following 72 hours separately from each other, using Extreme Learning Machines with Numerical Weather Predictions and series of past values as input. Therefore, two types of data were used in the proposed model:

- Numerical Weather Predictions;
- Historical data from the power plant power production.

The data comes from an undisclosed party, and includes both the NWP and the series of past values of the power production for the span of the year 2010.

In this chapter, firstly, a more insightful view over the NWP available for this thesis is given. Then, the forecasting model layout is presented in some detail. After this, the error measure techniques are presented.

5.1. Data used

The data used in this thesis refers to a real a real power plant located in southern Italy, with an installed power capacity around 5kW. The weather history data includes the following indexes: Global Irradiance, Direct Irradiance, Solar Altitude, Average Solar Altitude, and Temperature within 2 meters of the ground and the power produced for every hour of a year. As stated previously the data covers the span of a year, i.e. the span goes from January's 1st 2010 to December's 31th 2010.

Because the available data only covers the span of a year, a choice was made in order to scatter the testing data throughout the year instead of utilizing the last months. Therefore, the testing set is constituted by the months of April, August and December, and the training set encompasses the remaining months.

5.2.NWP Analysis

The Numerical Weather Predictions for this study were obtained by the ECMWF (European Centre of Medium-range Weather Forecasts) with a RAMS (Regional Atmospheric Modeling System) deterministic forecasting model at 00h UTC everyday for the next 72 hours for the period of the 2010 year.

In order to choose the most influential Numerical Weather Predictions for this case study, some tests will have to be done. One of the easiest ways the most relevant variables can be found is by scatter graphical analysis. So, some Power vs. several forecasted NWP scatter graphics will be presented next. At the end of this section Table 1 shows the forecasting errors.

In Figure 5.1 a scatter graphic between the power production and the forecasted Direct Normal Irradiance is presented. It can be seen that the data has a high variance and is a little sparse, but a certain level of correlation can be observed. Figure 5.2 shows a scatter graphic between power and measured DNI and a higher correlation is seen, as expected.

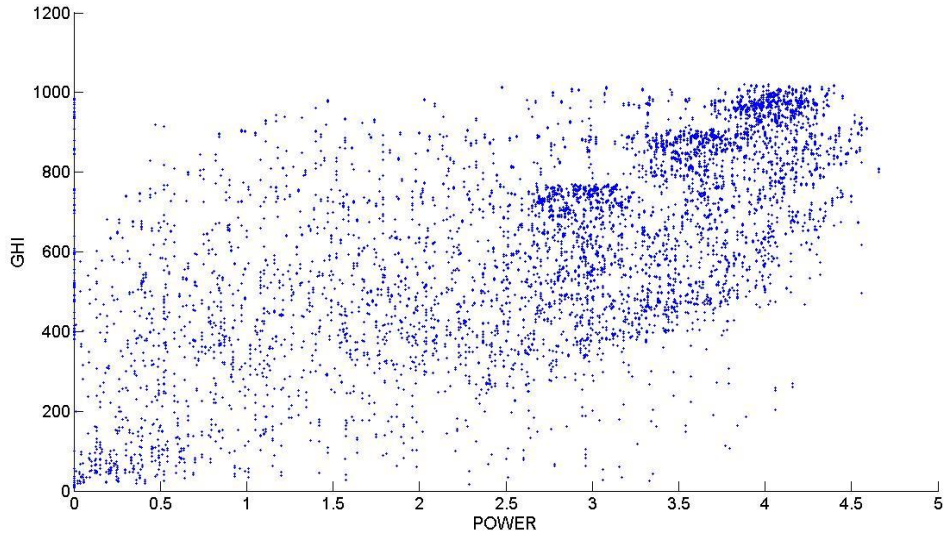

Figure 5.1 - Scatter graphic of Power vs. forecasted DNI

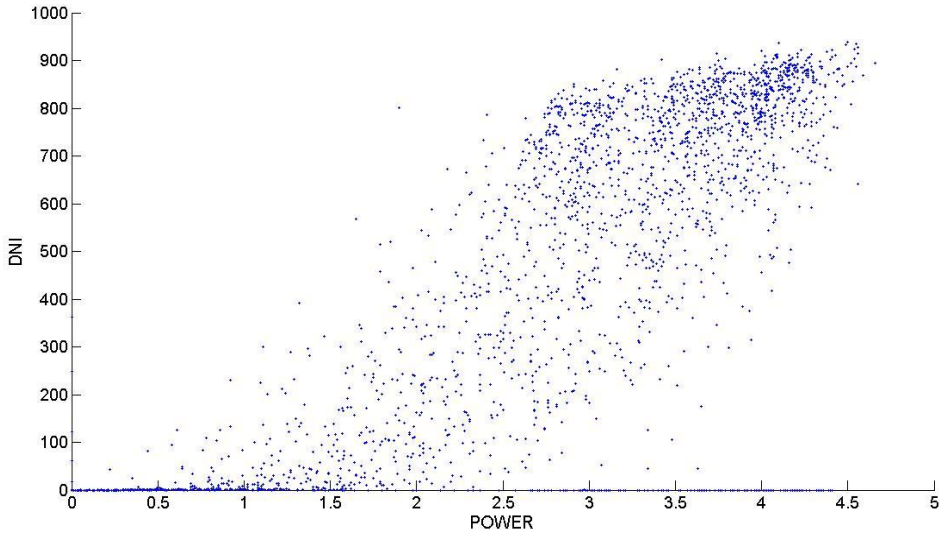

Figure 5.2 - Scatter graphic of Power vs. measured DNI

Figure 5.3 presents a scatter graphic between power production and the forecasted Global Horizontal irradiance is presented. Similarly to the previous case, the graphic is sparse with a high variance, although a correlation can be identified between both variables. Figure 5.4 shows the same variables but this time, instead of the forecasted GHI, the measured values are presented, and a significant difference is seen concerning the correlation of the variables.

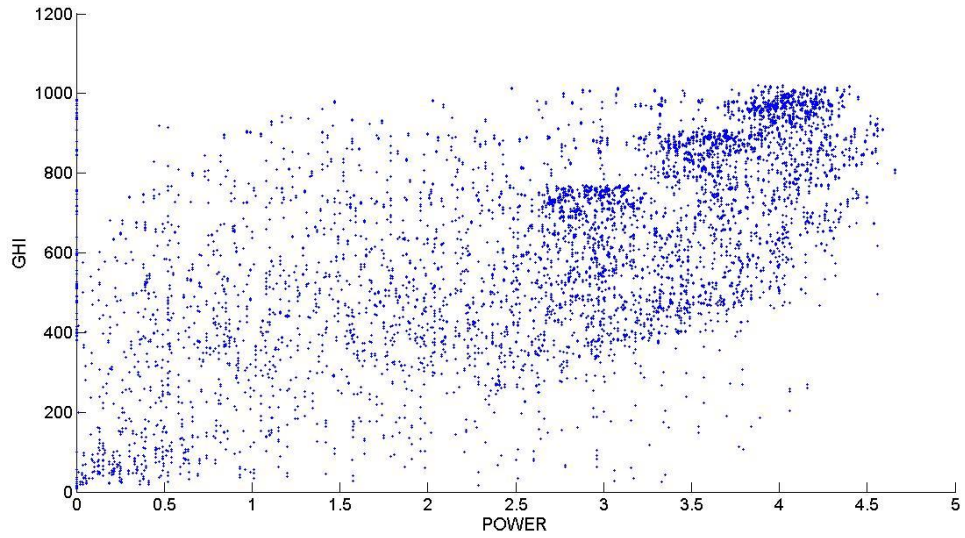

Figure 5.3 - Scatter graphic of Power vs. forecasted GHI

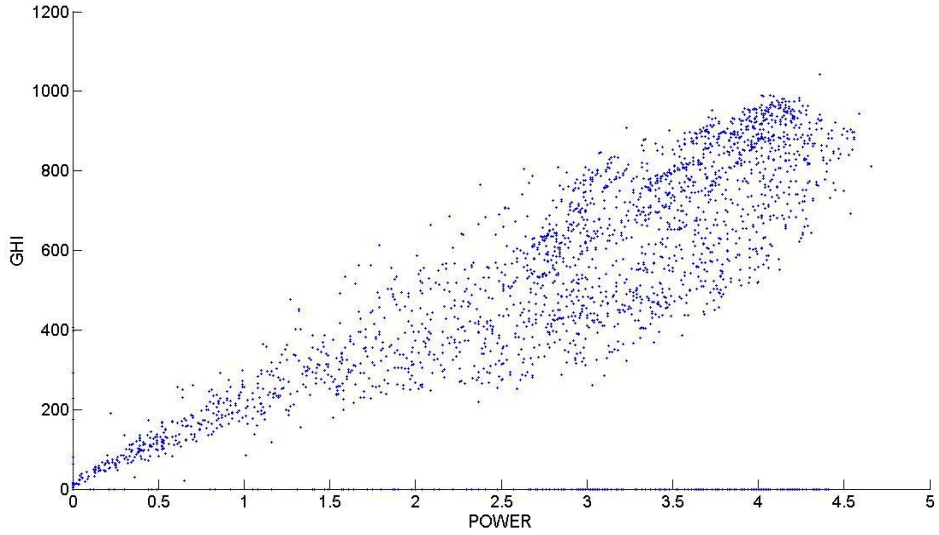

Figure 5.4 - Scatter graphic of Power vs. measured GHI

Another scatter graphic is shown in Figure 5.5, representing the relation between the power production and the forecasted cloudiness. A correlation between the variables is not easily identifiable once the graphic is very sparse. In this case, the measured values of cloudiness are not available, so those values cannot be compared.

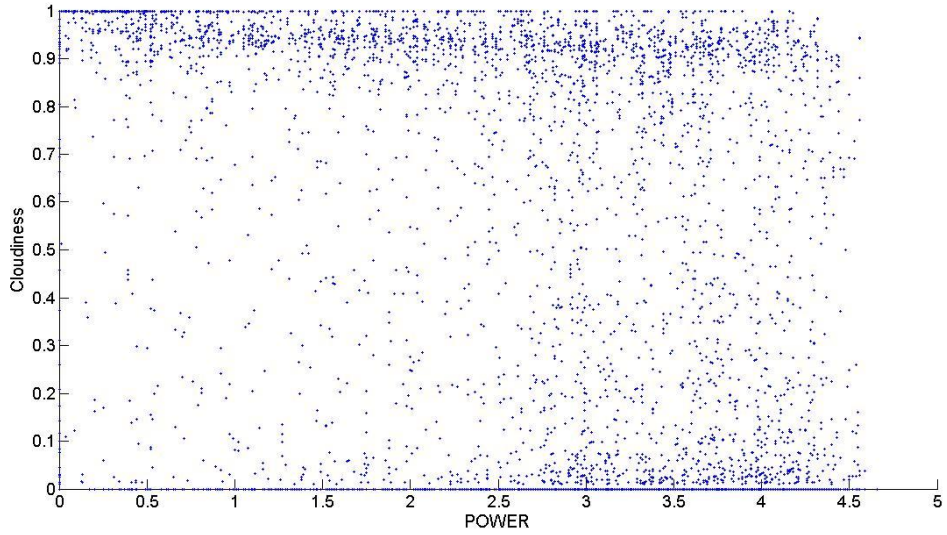

Figure 5.5 - Scatter graphic of Power vs. forecasted Cloudiness

The following graphic, presented in Figure 5.6, shows the correlation between the power production and the forecasted temperature 2 meter above ground level. Once again, it is hard to define a direct correlation between the variable since the data is very sparse, so further testing will be needed in order to achieve any conclusions. Figure 5.7 shows a scatter graphic between power and measured temperature 2 meters above ground. Although some correlation can be observed in the graphic, it is not completely visible.

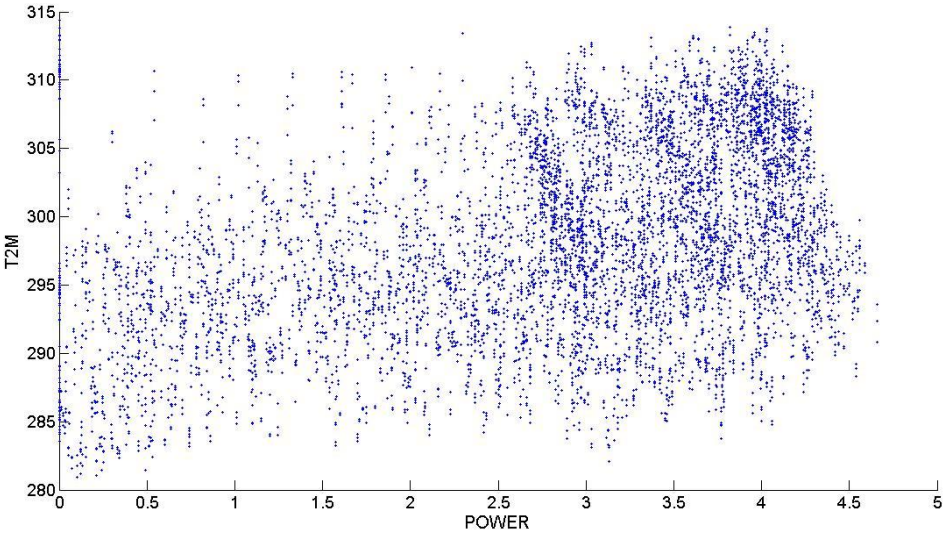

Figure 5.6 - Scatter graphic of Power vs. forecasted Temperature 2 meters above ground

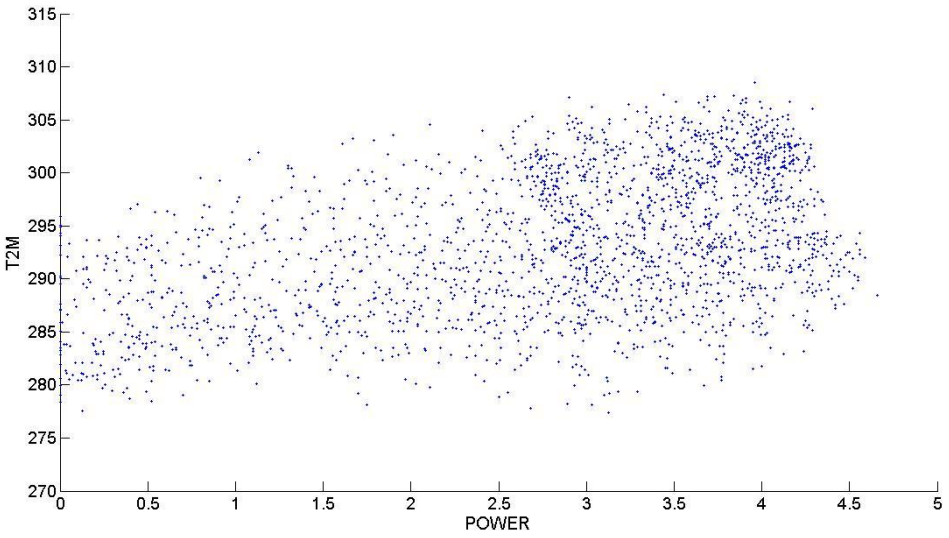

Figure 5.7 - Scatter graphic of Power vs. measured Temperature 2 meters above ground

Figure 5.8 exhibits the data relation between power production and solar altitude. Not many conclusions can be taken by the analysis of this graphic, as it shows great data variation and no direct correlation can be perceived. Finally, Figure 5.9 shows the power production is relation to the measured solar altitude. Since the solar altitude is not exactly a forecasted variable, once it can be calculated, both graphics are very similar, if not equal.

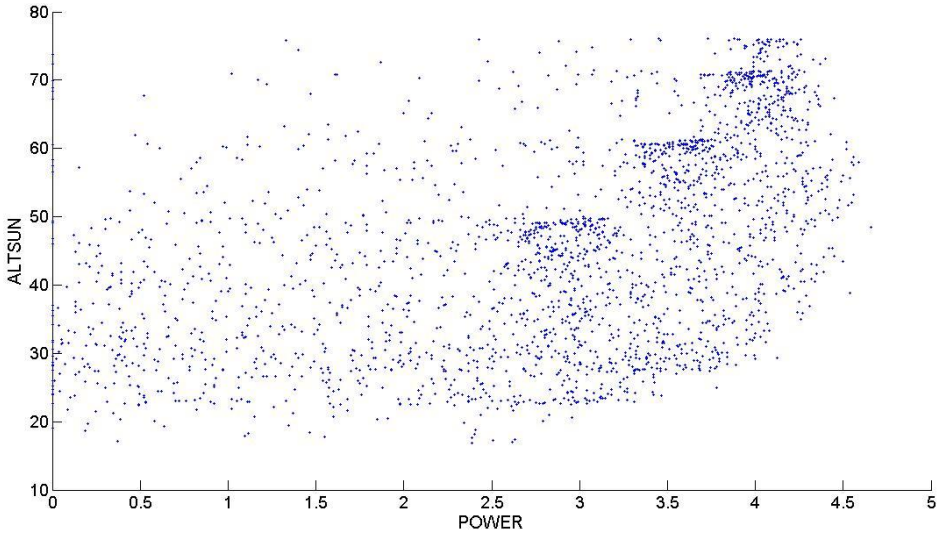

Figure 5.8 - Scatter graphic of Power vs. forecasted Solar Altitude

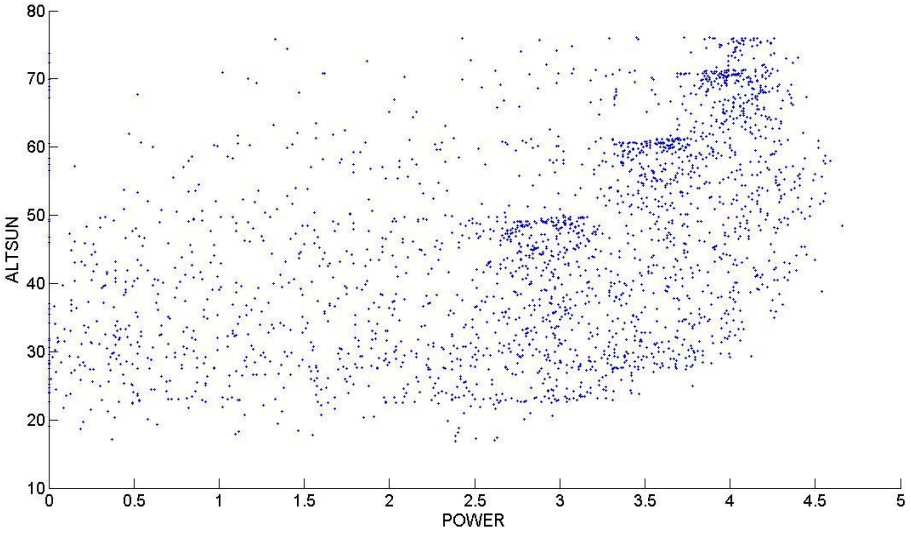

Figure 5.9 - Scatter graphic of Power vs. measured Solar Altitude

By analyzing the previous scatter graphics a conclusion can be reached that the direct correlation between the NWP forecasts and the power production of the Photovoltaic plant is not truly clear, once a great dispersion of the data can be observed. Even though, DNI and GHI seem to have the closest correlation with the power output. Although those two variables seem more fit and reliable to proceed the forecasting method, further testing with several variables available will be executed in order to reach the best combination for the case in question in this work. The variable testing will also be useful to discover and understand any non-linear connections existing between power production and the NWP available to the study.

Also, the forecasting error for the some NWP, more specifically, GHI and DNI was calculated, and the results achieved are presented in Table 1:

Table 1 – GHI, DNI and Temperature 2 meters above ground forecasting errors

NWP Forecasting Error (RMSE)	
GHI	15,575 %
DNI	26,987 %
Temperature	24,429 %

5.3. Error Measures

In this section the error measures utilized to evaluate the forecasting method are presented. The forecasting error is usually defined as being the difference between the real measured value for the power production and the forecast obtained by the forecasting method.

$$e_{t+k|t} = P_{t,k} - \hat{P}_{t,k}$$

It is commonly used, especially for final results evaluation, the normalized forecasting error:

$$\epsilon_{t+k|t} = \frac{P_{t,k} - \hat{P}_{t,k}}{P_{max}}$$

Being P_{max} the maximum value of production of the data set, sometimes the installed power of the plant or the average value of the data set can also be utilized.

All the error measurements are made hourly for the present model and two evaluation methods are used. The Root Mean Square Error (RMSE) and Mean Average Error (MAE) are the methods chosen to evaluate the model.

The Root Mean Square Error (RMSE) also known as Root Mean Square Deviation (RMSD) is frequently used as a measure of the difference between the predicted values and the real values observed from the environment which is being modeled. These individual differences are known as residuals and the RMSE aggregates them into a single measure.

The RMSE is defined by the following equation:

$$RMSE = \sqrt{\frac{\sum_{i=1}^{n}\left(P_{t,k} - \hat{P}_{t,k}\right)^2}{n}}$$

The RMSE can be used to compare the individual model performance to that of other predictive models.

The Mean Average Error (MAE) measures the average magnitude of the errors in a set of forecasts. It measures accuracy for continuous variables. In other words, the MAE is the average over the verification sample of the absolute values of the differences between forecast and the corresponding observation. Also, MAE is a linear score which means that all every single difference is weighted equally in the average [62].

The MAE is given by the following equation:

$$MAE = \frac{1}{N}\sum_{i=1}^{n}\left|P_{t,k} - \hat{P}_{t,k}\right|$$

The MAE and the RMSE can be utilized together to make a diagnosis of the variation of the errors in a given data set. The RMSE will always be larger or in some cases equal to the MAE, the greater the difference between both of them, the greater the variance in the individual errors in the data sample. If the RMSE is equal to the MAE, then all errors are of the same magnitude [62].

The normalization of these error measures are defined by the following equations:

$$NRMSE = \frac{\sqrt{\frac{\sum_{i=1}^{n}\left(P_{t,k} - \hat{P}_{t,k}\right)^2}{n}}}{P_{max}}$$

And,

$$NMAE = \frac{\frac{1}{N}\sum_{i=1}^{n}\left|P_{t,k} - \hat{P}_{t,k}\right|}{P_{max}}$$

An error is calculated for every hour of the time span, i.e., 72 different errors are calculated for each set of forecasts, giving an estimated error for each of the 72 hours which compose the forecasting time span.

5.4. Forecasting Model Evaluation

The performance and results of the developed method are compared against the measured data available for the data set. These measured variables were provided along with power production data for the whole year.

5.4.1. *Choosing the NWP forecasting set*

As stated above, the available Numerical Weather Predictions when analyzed only by the scatter graphics leave some gap to the existence of certain doubts whether they are relevant

to the present case or not. Therefore, some testing is needed in order to truly find if the Numerical Weather Predictions are indeed relevant or not.

As stated before in this document, the time series variable P_{t-1} is only used through the first 5 hours of the forecasting span, so a separation between the first 5 hours and the rest of the span will be made. The combinations were tested with several different number of hidden layer neurons in order to find the best fit.

The following Table 2 shows the results achieved in this matter:

Table 2 - NMAE for the test set for several combinations of NWP and the respective neurons which provided the best forecast for each case

		NMAE (%)					
NWP	Neurons	Hour 1	Hour 2	Hour 3	Hour 4	Hour 5	Hours 6-72
1. AltSun, GHI, DNI and Cloudiness	26	5,9778	8,1721	9,2125	9,5350	9,5915	11,5104
2. AltSun, GHI, DNI, Cloudiness, T2M	34	6,0702	8,5328	9,7165	10,0020	10,0033	11,4514
3. GHI, DNI, Cloudiness, T2M	26	6,3127	8,4765	9,2988	9,4640	9,3532	11,7785
4. GHI, DNI, Cloudiness	17	6,0004	8,1648	9,2521	9,5798	9,6740	11,5325
5. AltSun, GHI, DNI	17	5,9812	8,0920	9,0528	9,3884	9,6059	11,4114
6. GHI, DNI, T2M	17	6,0001	8,1951	9,2218	9,4064	9,4198	11,6440
7. GHI, DNI	12	5,9725	8,0743	9,0550	9,3482	9,5233	11,4363

As seen in Table 2, three hypotheses rise a little above the others, hypothesis 1, hypothesis 5 and hypothesis 7. It also can be seen that hypothesis 7 has marginally better results than the others, so the better combination of Numerical Weather Predictions for the case in question is a simple combination of Direct Normal Irradiance and Global Horizontal Irradiance.

These results correspond to the first impression when looking at the scatter graphics back in section 5.1. Those two variables, i.e. GHI and DNI are known as the most influential concerning PV power production forecasting, in this specific case they achieve better results when used alone than when joined by other variables.

5.4.2. *Choosing the Activation Function*

Section 4.6 presents several Activation Functions which frequently are, some more than others, used in forecasting methods. This section shows the results of the testing done with all the aforementioned Activation Functions for the present case.

This can be seen inTable 3 and Table 4 presented next:

Table 3 - Activation Function with corresponding NMAE (%)

Activation Function	*Hour 1*	*Hour 2*	*Hour 3*	*Hour 4*	*Hour 5*	*Hours 6-72*
Sigmoid	5,9725	8,0743	9,0550	9,3482	9,5233	11,4363
Sine	5,9805	8,1437	9,1790	9,4999	9,6553	11,4949
Hard Limit	6,0912	8,3512	9,3130	9,6012	9,7964	12,3289
Triangular basis	6,9319	9,6674	11,0856	11,9521	12,3118	17,9306
Radial basis	6,0173	8,2131	9,2271	9,5132	9,6218	11,8659

Table 4 - Activation Functions with corresponding Training and Testing Times (in seconds) and Neurons used to achieve the best results

Activation Function	*Neurons*	*Training Time*	*Testing Time*
Sigmoid	12	5,039	1,361
Sine	11	4,792	1,324
Hard Limit	12	4,656	1,262
Triangular Basis	10	4,051	1,201
Radial Basis	12	5,370	1,565

By analyzing Table 3and Table 4, the best results are achieved with the sigmoid and the sine functions as Activation Functions. Although the sigmoid function provides marginally better results than the sine function. The number of hidden layer neurons which provide the best results varies from one activation function to another, as seen above, although this variation is not abrupt.

In terms of training and testing speeds, the triangular basis function is somewhat faster than the rest others, but the results achieved with this function are the worst.

From this, a conclusion can be taken that the fittest Activation Function to use in this specific case is the Sigmoid Function.

5.4.3. *Forecasting Results*

As seen in the previous sections for the case of study of the present thesis, the best combination of Numerical Weather Predictions is the use of Global Horizontal Irradiance and Direct Normal Irradiance and the best Activation Function is the sigmoid function.

Thus, the following results were obtained with the use of aforementioned combination of variables. One particularity of the developed method is that it trains a network for each hour of the time span, and also it can start from whatever hour is chosen. The following examples start at different times of the day; the first two samples start at 00:00 UTC and the subsequent two start at 9.00 UTC for the 72 hour span. For the cases starting at 9:00 UTC the span does not cover the expected 72 hour span because no data is available past the third day of forecasting.

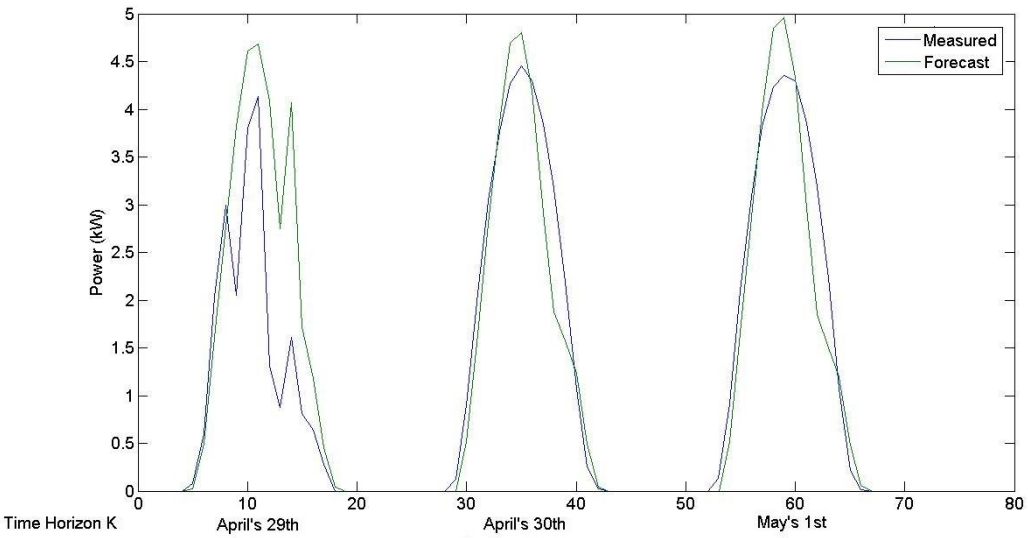

Figure 5.10 - Forecast made for April's 29th at 00:00 UTC for the next 3 days

Figure 5.10 shows a forecast made for April's 29th at 00:00 UTC for the next 3 days. In this figure the forecast's error is by excess, i.e. the forecasted values are greater than the measured values, when analyzing the NWP available for this horizon, the forecasted variables (DNI and GHI) are substantially higher than the measured ones, which leads to this error. This can be observed in Figure 5.11:

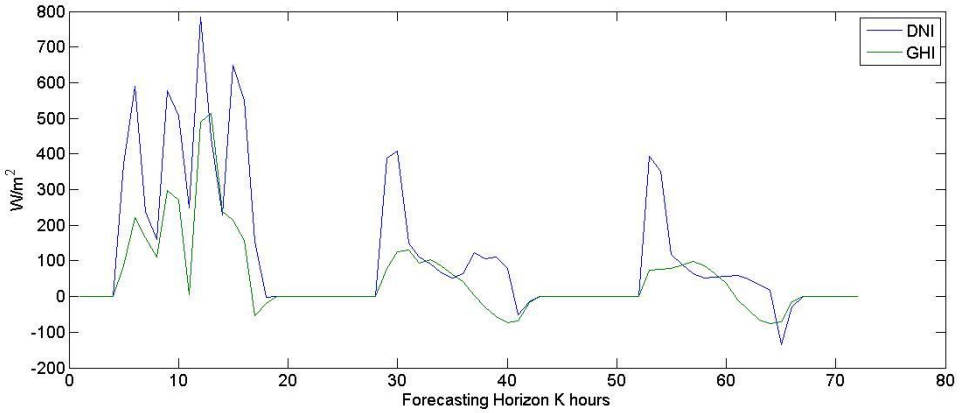

Figure 5.11 – Irradiation forecasting error for the span of April's 29th to May's 1st

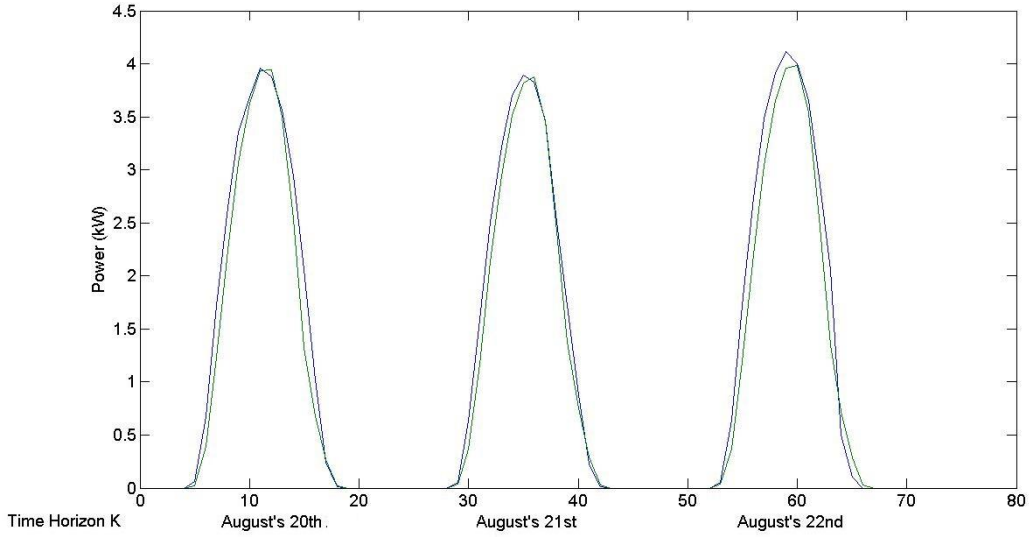

Figure 5.12 - Forecast made for August's 20th at 00:00 UTC for the next 3 days

Figure 5.12 shows a forecast made for August's 20th at 00:00 UTC for the next 3 days. This time span represents summer days with clear sky, and the forecast provides an almost null error, a small divergence can be seen in the forecast for August's 22nd, in which the produced power peaks a little higher than the forecast. This can be explained by analyzing the previous days, once the forecasting model utilizes series of past values and the previous day's peak is lower than in that day.

The next set of figures will show forecasts starting at 9:00 UTC:

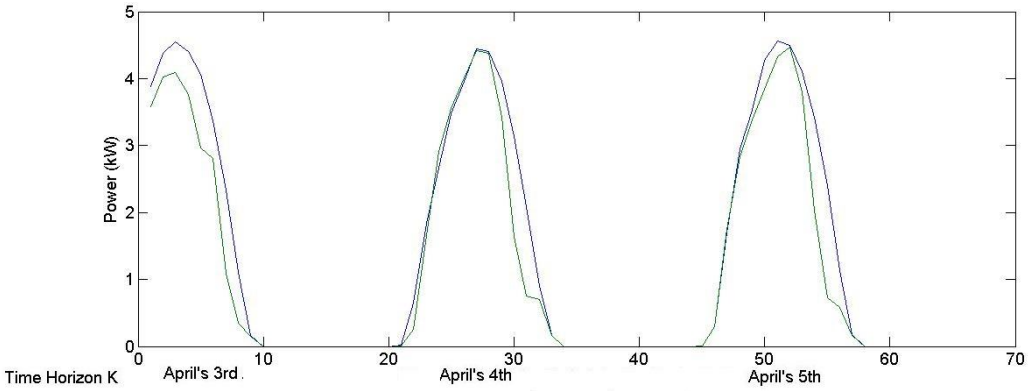

Figure 5.13 - Forecast made for April's 3rd at 9:00 UTC for the next three days

Figure 5.13 shows a forecast made for April's 3rd for the next 3 days, starting at 9:00 UTC. In this case, the NWP present a negative error, i.e. the NWP are lower than the measured values, mostly for the second half of the day which leads to the graphic seen above. The error can be observed in Figure 5.14:

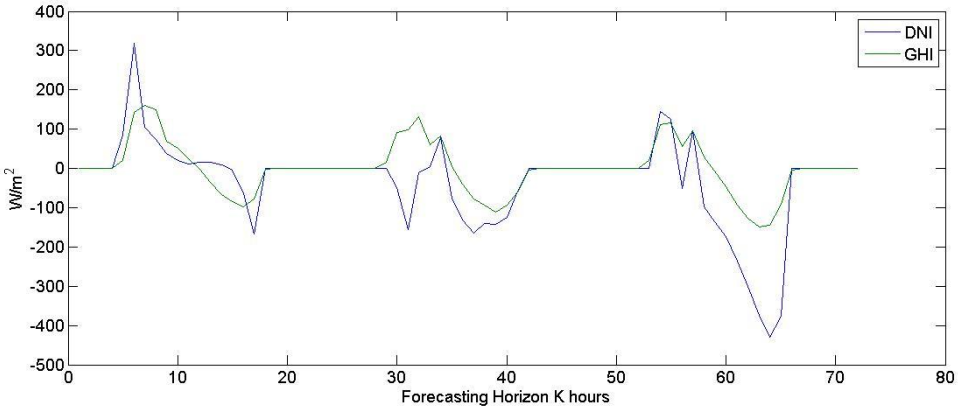

Figure 5.14 – Irradiation forecasting error for the span of April's 3rd to April's 5th

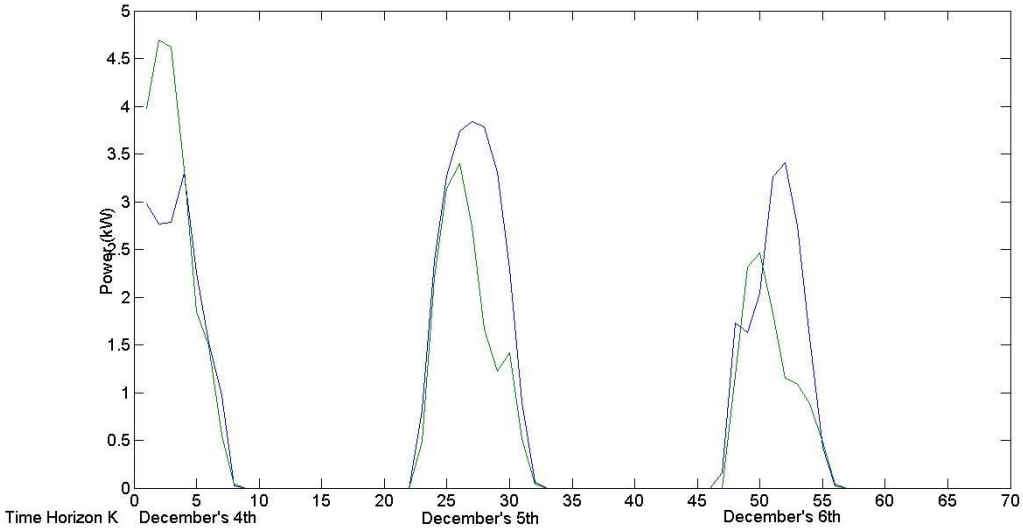

Figure 5.15 - Forecast made for December's 4th at 9:00 UTC for the next three days

Figure 5.15 shows a forecast made for December's 4th for the next 3 days, starting at 9:00 UTC. The choice of the 9:00 UTC hour relates to the hour of opening of the power trade market, in this case the MIBEL. One again, the NWPs have a relatively high error which affects the final results of the forecasting. Figure 5.16 shows the NWP error:

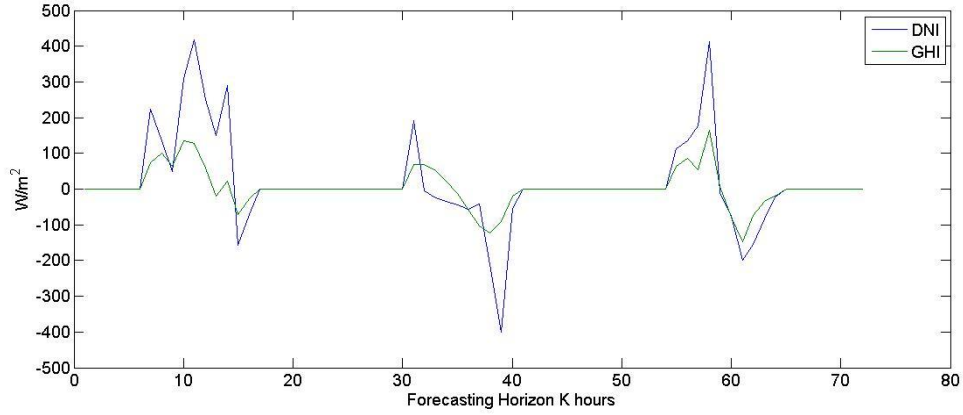

Figure 5.16 – Irradiation forecasting error for the span of December's 4th to December's 6th

The figures above show that, as expected, in clear sky days, when the solar irradiance does not vary too much, the achieved results are fairly good, but when the solar irradiance shows some oscillation the forecast gets worse.

5.5. Forecasting Model performance

Apart from the original hybrid ELM model proposed for this thesis, in order have a better perception over the achieved results, a comparison with a purely Autoregressive model (which do not use NWP) and an ELM model using only NWP data.

The achieved results can be seen below:

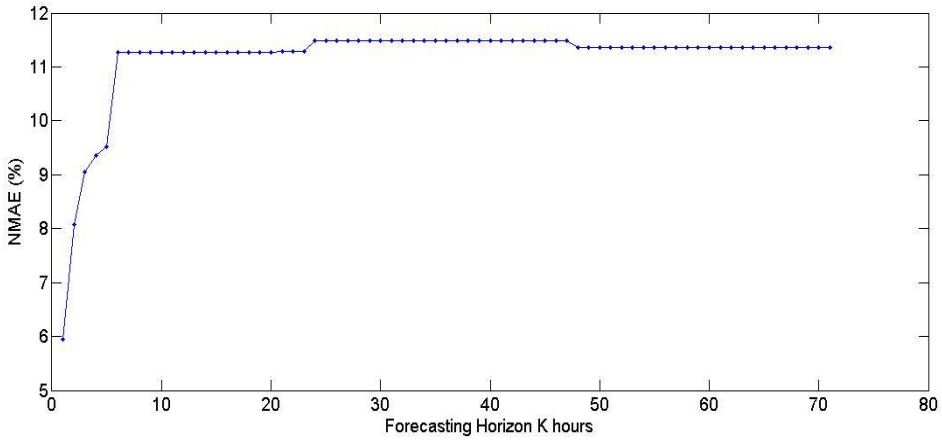

Figure 5.17 - NMAE vs. Forecasting Horizon for the Hybrid ELM model

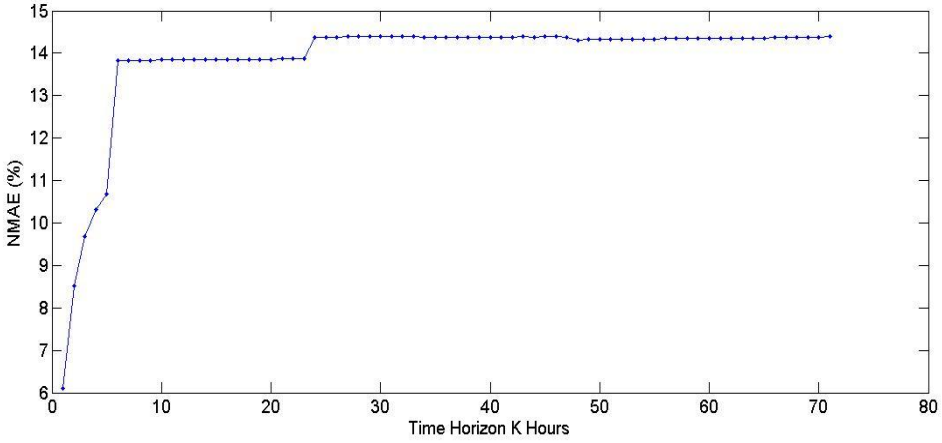

Figure 5.18 - NMAE vs. Forecasting Horizon for Autoregressive ELM model

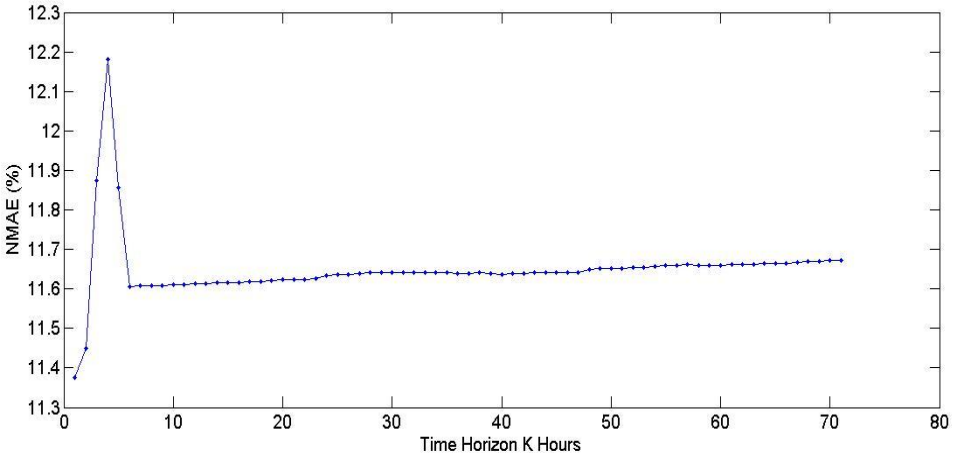

Figure 5.19 - NMAE vs. Forecasting Horizon for the NWP ELM model

Figure 5.17 shows the NMAE of the hybrid model, the error is lower for the 5 first hours due to the use of $P_{t_{-1}}$ past time series, as stated previously.

Figure 5.18 shows the error values for the autogressive model, when comparing with the hybrid model, it is noticeable that the shape of the graphic is identical, but the error is higher, this is due to the use of NWP in the hybrid model, which lowers the error.

Figure 5.19 shows the NMAE when using only NWP with the ELM model, once the series of past values are not used in this model, the input for the model do not differ much from each other, thus, the low variation of the error for the whole span of time, i.e. the difference between the higher error and the lower is very small being this difference observed in the first hours of the time span. From this one can deduce that for the first hours of the time span, the series of past values are more important than the NWP.

5.6. Comparison with other Methods

This section presents a comparison between the Extreme Learning Machines proposed model, and Artificial Neural Networks and Support vector Machines.

Table 5 shows the test errors obtained with the same data set for the different methods. The ELM developed method provided better results than the other two methods. The ANN is slightly worse than the ELM; The ANN was trained and tested with the Levenberg-Marquardt algorithm with Mat Lab. For the SVM the Mat Lab library LIBSVM was used, once it does not possess any native function for this method. The worst results were obtained by the SVM model. The present results are the mean of 50 runs of each model.

Table 5 - NMAE (in percentage) for the referred statistical models

Method	*Hour 1*	*Hour 2*	*Hour 3*	*Hour 4*	*Hour 5*	*Hours 6-72*
ELM	5,9725	8,0743	9,0550	9,3482	9,5233	11,4363
ANN	6,3472	8,9305	8,7815	9,3619	9,5729	11,9463
SVM	8,1652	10,0673	10,6902	11,1738	10,4920	12,2741

In terms of speed, the ELM is much faster than the other two models; Table 6 shows the times for one run of each model in an Intel Core i7 Q720 @ 1.60 GHz with 8GB of RAM:

Table 6 - Training and Testing times of the statistical methods (in seconds)

Method	*Training Time*	*Testing Time*
ELM	5.039	1.361
ANN	15.929	1.3731
SVM	37.147	7.941

As seen above, the Extreme Learning Machines model achieves very good performances even when comparing with other statistical methods. Most glaringly is its speed which completely overwhelms the other models.

The errors can be graphically seen below in Figure 5.20 and Figure 5.21:

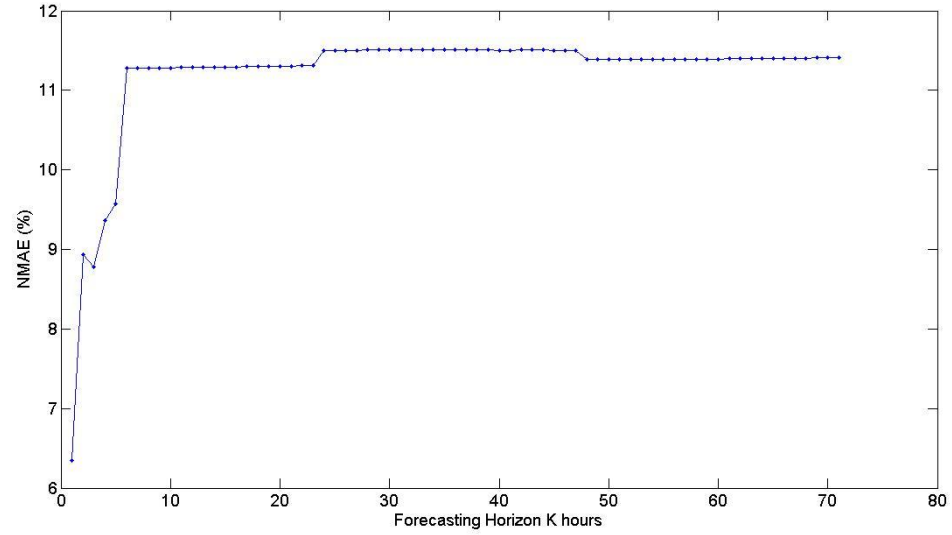

Figure 5.20 - NMAE vs. Forecasting Horizon for the ANN model

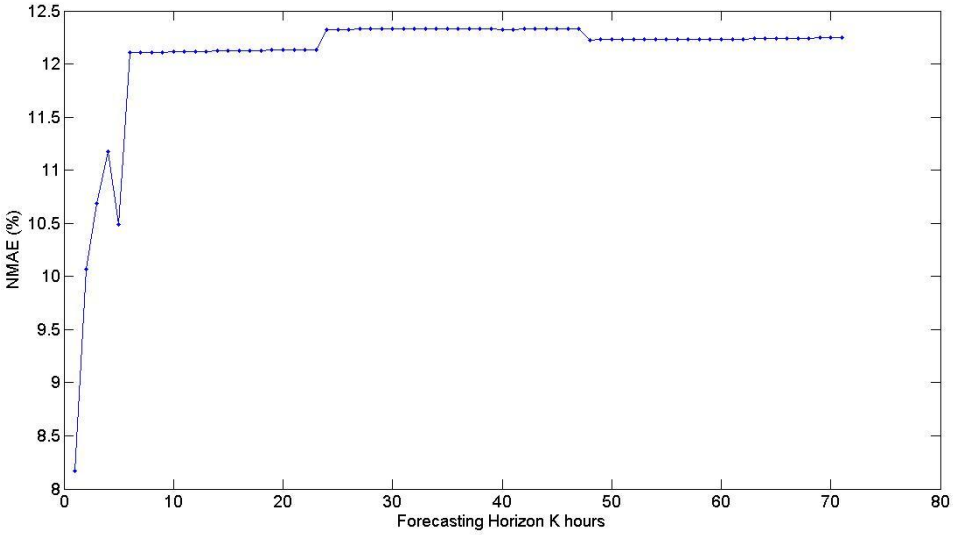

Figure 5.21 - NMAE vs. Forecasting Horizon for the SVM model

Chapter 6

Conclusion

Although the Photovoltaic energy production has not yet an expressive share when compared to traditional sources, it is estimated, as seen previously, that it will rise in importance in the coming years. This kind of energy has insurmountable capabilities to explore, and is the biggest source of energy mankind has access to. Also, the continuous pressures of environmental institutions backed by Kyoto's protocol, makes it a priority to develop and increase the use of renewable energies. Thus, power production forecasting is increasingly gaining importance, as a tool to improve the control capability and usability of these energies, once they are very intermittent and hard to predict.

The main objective of the present thesis was to develop a new and innovative forecasting method, for short-term photovoltaic forecasting, in this case for a span of 72 hours ahead. The main conclusions are presented next.

A method for photovoltaic power production forecasting has been developed using a relatively new technology called Extreme Learning Machines. The developed method forecasts the photovoltaic power production for the next 72 hours, and a forecast is made for each hour of the span, i.e. 72 different networks were trained and tested. One particularity of the present method is the capability of varying the starting hour of the forecast, i.e. it can start at 0:00 UTC or at 9:00 UTC or at which hour it is preferred or suits better the user.

The method focused on Extreme Learning Machines algorithms analyzed three different forecasting models: One using only data of production past values, i.e. purely autoregressive; another using only Numerical Weather Predictions; and the last one being a hybrid model between the two previously referred models, i.e. using series of past values and NWP. The conclusion was that the hybrid model provides better results, which infers that the use of NWP enhances the results and thus, they add value to the forecasting model.

Also, several NWP variables were tested in order to find the best combination for the present method. The available variables were temperature 2 meters above ground, direct normal

irradiance, global horizontal irradiance, cloudiness and solar altitude. It was found that the minimum forecasting error was obtained when a conjugation of direct normal irradiance and global horizontal irradiance was used.

Several activation functions were also tested with the developed model and the best results were achieved when using the sigmoid function.

The developed model was also tested against other statistical models, e.g. ANN and SVM, and better results were achieved when using the same data sets for each model. The ANN obtains slightly worse results than the ELM, while the SVM is clearly the less reliable model in this case. Also, one important feature of the Extreme Learning Machines relating to other methods is its learning speed, which overwhelms the other models. Learning speed is very important characteristic for forecasting models, once it very important that the forecast are ready before the opening of the markets, and thus, the forecasts cannot take too much time to be done.

The available data set for this thesis covers only the span of one year (2010), which is not ideal for this kind of work. To try to lessen the influence of this detail, the training and testing sets were rearranged in order to avoid training the model with mostly summer and spring months and testing with autumn and winter months.

The objectives of the proposed thesis were entirely covered and fulfilled. A forecasting model of Extreme Learning Machines using a hybrid combination of series of past values and NWP was develop and tested, and the results were found fairly good, reaching an error below 6% for the first hour and steadily rising to around 9% for the following 4 hours, once they use series of past power production values as input, for the span of the hours 6-72 the Numerical Weather Predictions were found to be a more relevant input with an error always rounding 11%. Nevertheless further work can be done to improve the model.

6.1. Future Works

For future works some possibilities are presented:

- Calculation of the diffuse radiation in order to add more precision to the method;
- Calculation of the temperature of the PV module from the ambient temperature;

- Using other NWP variables as input in order to test their influence, e.g. wind speed or wind direction could be of influence;
- The creation of an user interface could also had value to the developed method once it would be easier to use;
- Data of several years could be used in order to find a better characterization of seasonal periodicity.

Bibliography

[1] Bacher, Peder, "Online Short-term Solar Power Forecasting", Solar Energy 83, 1772-1783 Accessed in September 2013.

[2] Neves, Ricardo, "Desenvolvimento de modelos de previsão de produção de centrais fotovoltaicas". Accessed in September 2013.

[3] http://www.ntu.edu.sg/home/egbhuang/ , Accessed in September 2013

[4] http://cleantechnica.com/2013/10/08/advantages-disadvantages-solar-power/ , Accessed in October 2013

[5] http://www.erse.pt , Accessed in October 2013

[6] http://expresso.sapo.pt/renovaveis-abastecem-portugal-de-eletricidade=f797507, Accessed in October 2013

[7] http://www.indexmundi.com/blog/index.php/2013/08/07/china-at-the-top-of-renewable-energy-investment/ October 2013

[8] http://www.carbonbrief.org/blog/2013/01/renewable-investment-drops-2012/, Accessed in October 2013

[9] http://cleantechnica.com/2013/07/12/solar-pv-to-hit-grid-parity-134-billion-annual-revenue-by-2020/, Accessed in October 2013

[10] http://www.3tier.com/en/support/resource-maps/, Accessed in October 2013

[11] Monteiro, Cláudio, "Previsão de Consumos – O problema da previsão de consumos", Available in http://paginas.fe.up.pt/~cdm/DE2/DE2_A3a.pdf , Accessed in October 2013

[12] Sousa, João, http://www.slideshare.net/CongressoEnergiaViana/joo-sousa-prewind , Accessed in October 2013

[13] http://www.cmhc-schl.gc.ca/en/co/grho/grho_009.cfm , Accessed in October 2013

[14] http://www.fsec.ucf.edu/en/consumer/solar_electricity/basics/how_pv_system_works.htm , Accessed in October 2013

[15] Centro de Referência para Energia Solar e Eólica Sérgio de Salvo Brito, "Energia Solar - Princípios e Aplicações"., Accessed in October 2013

[16] "Energia Fotovoltaica – Manual sobre tecnologias", projecto e instalação, http://www.jgduarte.com/download/greenpro_fotovoltaico.pdf, Accessed in October 2013

[17] http://www.yourhome.gov.au/technical/fs67.html, Accessed in October 2013

[18] Hyndman, Rob J., Athanasopoulos, George, "Forecasting: Principles and practice", http://www.otexts.org/book/fpp, Accessed in October 2013

[19] Sfetsos, A., Coonick, A.H., "Univariate and Multivariate Forecasting of Hourly Solar Radiation With Artificial Intelligence Techniques", Solar Energy, 2000. 68(2) p.129-134, Accessed in November 2013

[20]Box, George E.P.; Jenkins, Gwimly M.; Reinsel, Gregory C., "Time Series Analysis: Forecasting Control", Prentice-Hall Inc., Accessed in November 2013

[21]Heineman, Detlev; Lorenz, Elke; Girodo, Marco; "Forecasting of Solar Radiation", Solar Energy 67, 139-150, Accessed in November 2013

[22]Wu, Ji; Chan, Chee Keong; "Prediction of hourly solar radiation using a novel hybrid model of ARMA and TDNN", Accessed in November 2013

[23]Heineman, Detlev; Lorenz, Elke; Girodo, Marco; "Solar irradiance forecasting for the management of solar energy systems", Solar 2006, Denver, CO, USA, Accessed in November 2013

[24]Silva, Carlos, "Desenvolvimento de uma metodologia e ferramentas para a previsão da produção elétrica em parques fotovoltaicos", Accessed in November 2013

[25] Zhang, G et al.,"Forecasting with artificial neural networks", Accessed in November 2013

[26]Krogh, Anders, "What are artificial neural networks", Available in http://www.apl.jhu.edu/~przytyck/neural_net_primer.pdf, accessed in November 2013

[27]http://www.learnartificialneuralnetworks.com/ , Accessed in November 2013

[28]Aamodt, Rune, "Using artificial networks to forecast financial time series", Available in http://www.diva-portal.org/smash/get/diva2:353048/FULLTEXT01.pdf, Accessed in November 2013

[29]http://iticsoftware.com/forex-neural-backpropagation, Accessed in November 2013

[30]http://upload.wikimedia.org/wikipedia/commons/7/73/AtmosphericModelSchematic.png , Accessed in November 2013

[31]http://reference.wolfram.com/applications/neuralnetworks/NeuralNetworkTheory/2.5.1.html, Accessed in November 2013

[32]http://www.roguewave.com/portals/0/products/imsl-numerical-libraries/c-library/docs/7.0/html/cstat/default.htm?turl=multilayerfeedforwardneuralnetworks.htm , Accessed in November 2013

[33]Joachims, Thorsten, "Text categorization with support vector machines: Learning with many relevant features", Available in http://link.springer.com/chapter/10.1007/BFb0026683#page-1, Accessed in November 2013

[34]Basak, Debasish et al., "Support Vector Regression", Available in http://pdf.aminer.org/000/260/306/position_control_of_ultrasonic_motor_using_support_vector_regression.pdf, Accessed in November 2013

[35]Hammer, A. et al., "Solar energy assessment using remote sensing techniques", Remote Sensing of Environment 86, 423-432, 2003, Accessed in January 2013

[36]Huang,Guang-Bin, Siew, Chee-Kheong, "Extreme learning Machine with Randomly Assigned RBF Kernels", International Journal of Information Technology, Vol. 11, No. 1, pp: 16-24, 2005. Accessed in November 2013

[37]Huang, G.; Zhou, H.; Ding,X.; et al.; “Extreme Learning Machines for regression and multiclass classification.”, Accessed November 2013

[38]Liu, Quige; He, Qing; Shi, Zhongzhi; “Extreme Support Vector Machine Classifier”, Accessed in December 2013

[39]Huang, G.; Zhu, Q.; Siew, C.; “Extreme Learning Machine: Theory and applications”, Neurocomputing, Vol. 70, pp: 489-501, 2006 Accessed in December 2013

[40]Frénay, Benoît; Verleysen, Michel; “Using SVMs with randomized feature spaces an extreme learning approach”, Accessed in December 2013

[41]Suykens, J.A.K.; Vandewalle, J.; “Training multilayer perceptron classifiers based on a modified support vector method”, Accessed in December 2013

[42]Huang, G.; Zhou, H.; Ding,X.; “Optimization method based extreme learning machine for classification”,Accessed in December 2013

[43]Bartlett, P.L.; “ The sample complexity of pattern classification with neural networks: The size of the weights is more important than the size of the network”, Accessed in December 2013

[44]http://www.3tier.com/en/support/solar-prospecting-tools/what-global-horizontal-irradiance-solar-prospecting/, Accessed in December 2013

[45]http://pvpmc.org/modeling-steps/irradiance-and-weather-2/irradiance-and-insolation/global-horizontal-irradiance/, Accessed in December 2013

[46]http://www.brighton-webs.co.uk/energy/solar_horizontal_surface.aspx, Accessed in December 2013

[47]http://www.bom.gov.au/climate/austmaps/solar-radiation-glossary.shtml, Accessed in December 2013

[48]http://www.3tier.com/en/support/solar-prospecting-tools/what-direct-normal-irradiance-solar-prospecting/, Accessed in December 2013

[49]Dai, Aiguo, et al.; “Recent trends in cloudiness over the united states: A tale of monitoring inadequencies”, Available in http://www.cgd.ucar.edu/cas/adai/papers/Dai_etal_BAMS_Clouds.pdf, Accessed in December 2013

[50]Mantzari, Vassilili H.; Mantzaris, Dimitrios H.; “Solar Radiation: Cloudiness forecasting using a soft computing approach”, Accessed in December 2013

[51]http://pveducation.org/pvcdrom/properties-of-sunlight/elevation-angle, accessed in December 2013

[52]Soteris A, K., “Applications of artificial neural-networks for energy systems. Applied Energy”, Applied Energy, 2000. 67(1-2): p. 17-35, Accessed in December 2013

[53]Ogliari, E., et al., “Hybrid Predictive Models for Accurate Forecasting in PV Systems”, Accessed in December 2013

[54]Yona, A.; Senjyu, T.; Saber, A.Y.; Funabashi, T.; Sekine, H.; Kim, C.-H. “Application of Neural Network to One-day-ahead 24 hours Generating Power Forecasting for Photovoltaic System.”, Accessed in December 2013

[55]Zeng, J; Qiao, W; “Short-term solar power prediction using a support vector machine”, Accessed in December 2013

[56]Huang, G et al.; “Extreme Learning Machine: A New Learning Scheme of Feedforward Neural Networks”, International Joint Conference on Neural Networks, Vol. 2, pp: 985-990, 2004, Accessed in December 2013

[57]“The Moore-Penrose pseudo-inverse”, Available in http://robotics.caltech.edu/~jwb/courses/ME115/handouts/pseudo.pdf, Accessed in December 2013

[58]“Neural activation functions”, Available in http://staff.science.uva.nl/~leo/math/sigma.pdf, Accessed in December 2013

[59]I.S.Isa, Z.Saad, S.Omar, M.K.Osman, K.A.Ahmad, H.A.Mat Sakim, “Suitable MLP Network Activation Functions for Breast Cancer and Thyroid Disease Detection”, Accessed in December 2013

[60]Bekir Karlik, A. Vehbi Olgac; “Performance Analysis of Various Activation Functions in Generalized MLP Architectures of Neural Networks”, Accessed in December 2013

[61]Muhammad Taher Abuelma'Att, Abdullah Bakri Shwehneh; "A Reconfigurable Gaussian/triangular Basis Functions Computation Circuit”, Accessed in December 2013

[62]http://www.eumetcal.org/resources/ukmeteocal/verification/www/english/msg/ver_cont_var/uos3/uos3_ko1.htm, Accessed in December 2013

[63]B. H. Chowdhury and S. Rahman, "Forecasting sub-hourly solar irradiance for prediction of photovoltaic output", in Conference Record of the IEEE Photovoltaic Specialists Conference, pp. 171-176, (1987), Accessed in December 2013

[64]S. Hokoi, et al., "Stochastic models of solar radiation and outdoor temperature", in ASHRAE Transactions Vol. 2, pp.245-252, Accessed in December 2013

[65]Mathiesen and Kleissl, “Evaluation of numerical weather prediction for intra-day solar forecasting in the continental United States”, Solar Energy 85 (5), 967-977, Accessed in December 2013

[66]Claudio Monteiro et al., “Short-Term Power Forecasting Model for Photovoltaic Plants Based on Historical Similarity”, Accessed in December 2013~

[67]Diagne et al., “solar irradiation forecasting: state of the art and proposition for future developments for small-scale insular grids”, Accessed in December 2013

[68]Paoli et al., “ Forecasting of preprocessed daily solar radiation time series using neural networks”, Solar Energy 84 (12), 2146-2160 Accessed in December 2013

[69]Mellit, Adel; Pavan, A.M.; “A 24h forecast of solar irradiance using artificial neural network: Application of performance prediction of a grid-connected PV plant at Trieste, Italy”, Solar Energy 84 (5), 807-821, Accessed in December 2013

[70]Lorenz, E., et al.; “Irradiance forecasting for the power prediction of grid-connected photovoltaic system”, IEEE Journal of Selected Topics in Applied Earth Observations and remote sensing, Vol. 2, No. 1, March 2009, Accessed December 2013

[71]http://science.howstuffworks.com/dictionary/physics-terms/heat-info3.htm, Accessed in December 2013

[72]Kwok, J.T.Y.;”Support Vector Mixture for Classification and Regression Problems”, Accessed in December 2013

[73]Rajesh, R.; Prakash, J.S.;”Extreme Learning Machines – A Review and State-of-the-Art”, Accessed in December 2013

[74]Reikard, G.;”Predicting Solar Radiation at High Resolutions: A Comparison of Time Series Forecasts”, Solar Energy 83 (3), 342-349, Accessed in December 2013

[75] Hamilton, J.D.;”Time Series Analysis” Princeton University Press, 1994, Accessed in December 2013

[76] Remund et al.;”Comparison of solar radiation forecasts for the USA”, Solar Radiation at High Resolutions: A Comparison of Time Series Forecasts”, USA. Proc. of the 23rd European PV Conference, 1.9-4.9 2008, Valencia, Spain Accessed in December 2013

[77]Perez et al.;”Validation of short and medium term operational solar radiation forecasts in the US”, Solar Energy 84 (5) 2161-2172, Accessed in December 2013

[78]Cao and Cao;”Forecast of solar irradiance using recurrent neural networks combined with wavelet analysis”, Energy 31, 3435-3445 (2006), Accessed in December 2013

[79]Lorenz et al.;”Benchmarking of different approaches to forecast solar irradiance”, In: Proceedings of 24 European Photovoltaic and Solar Energy Conference and Exhibition, Hamburg (Germany), Accessed in December 2013

[80]http://www.altenergystocks.com/archives/2012/04/five_more_winners_of_the_clean_energy_race_1.html , Accessed in January 2014

Appendixes

Appendix A

Clear Sky Model

The clear sky model used in this work was inspired by the one proposed by Bacher [1].

A clear sky model is normally a model which estimates the global irradiance in clear sky at any given time. Chowdhury and Rahman [63] divide the global irradiance into a clear sky element and a cloud cover element by:

$$G = G_{cs}.\tau_c$$

Where G is the global irradiance in W/m^2, G_{cs} is the clear sky global irradiance in W/m^2 and τ_c is the transmissivity of the clouds which they model as a stochastic process using ARIMA models. The clear sky global irradiance is found by

$$G_{cs} = I_0.\tau_a$$

Where I_0 is the extraterrestrial irradiance in W/m^2 and τ_a is the total sky transmissivity in clear sky, which is modeled by atmospheric dependent parametrization.

In the study proposed by Bacher [1], an identical approach is made, although instead of applying the factor on global irradiance it is applied to solar power, i.e.

$$p = p_{cs}.\tau$$

Where p is the solar power in W, p_{cs} is the clear sky power in W and τ is much like τ_c but since the clear sky model developed by Bacher [1] estimates p_{cs} by statistical smoothing

techniques rather than physics, the method can be mainly viewed as a statistical normalization technique and τ is then referred to as normalized solar power.

The main motivation behind this normalization of solar power with a clear sky model is that normalized solar power is more stationary than the solar power, so that classical time series models assuming stationarity can be used for predicting the normalized values.

The clear sky model is defined as:

$$p_{cs} = f_{max}(x, y)$$

Where p_{cs} is the clear sky solar power in W, x is the day of the year and y is the time of the day. The function $f_{max}(.,.)$ is assumed to be a smooth function and thus, can be estimated as a local maximum. The estimated clear sky function $\hat{f}_{max}(.,.)$ is then used to form the output of the clear sky model as the time series

$$\{\hat{p}_t^{cs}, t = 1, \dots, N\},$$

Where $\hat{p}_t^{cs}$ is the estimated clear sky solar power in W at time t and N is the number of hours of the time series. The normalized solar power Is then defined as

$$\tau_t = \frac{p_t}{\hat{p}_t^{cs}}$$

And this is used to form time series of normalized solar power.

For each (x,y) corresponding to the solar power observation p_t, weighted quantile regression estimates q quantile by a Gaussian two-dimensional smoothing kernel. The smoothing kernel is used to form the weights applied in the quantile regression. The applied weights are finally found by multiplying the weights from the two dimensions. The choice of quantile level q to be estimated and the bandwidth in each dimension, $h_x$and h_y, is based on a visual inspection of the results. A level of q = 0.85 was used.

For small $\hat{p}_t^{cs}$ values, the error of τ_t is naturally increasing and at nighttime the error is infinite. Therefore, all values of $\hat{p}_t^{cs}$ where

$$\frac{\hat{p}_t^{cs}}{\max(\{\hat{p}_t^{cs}\})} < 0.2$$

Are removed from $\{\tau_t\}$. $\max(\{\hat{p}_t^{cs}\})$ is the maximum value of the $\hat{p}_t^{cs}$ series.

The estimates of clear sky solar power are comprehensibly better in the summer period. The bad estimates in the winter periods are caused by the sparse number of clear sky observations.

It is noted that the deterministic changes of solar power are really caused by the geometric relation between the earth and the sun, which can be represented by the sun elevation as x and the sun azimuth as y.

Appendix B

Moore-Penrose generalized inverse matrix

The Moore-Penrose pseudo-inverse is a general way of finding a solution to the subsequent system of linear equations:

$$b = Ay \qquad b\epsilon\mathbb{R}^m; y\epsilon\mathbb{R}^n;\ A\epsilon\mathbb{R}^{mxn}$$

Moore and Penrose showed that there is a general solution for the latter equation system of the form of $y = A^{\intercal}b$. The matrix $A^{\intercal}$is the Moore-Penrose pseudo-inverse, and it was proved that is the unique matrix capable of satisfying the following properties:

- A$A^{\intercal}$A =A;
- $A^{\intercal}$A$A^{\intercal}$ = $A^{\intercal}$;
- (A$A^{\intercal}$)^T = A$A^{\intercal}$;
- ($A^{\intercal}$A)^T = $A^{\intercal}$A.

The Moore-Penrose pseudo-inverse has the following properties:

- m=n, $A^{\intercal} = \mathrm{A}$ if A is full rank. The pseudo-inverse for the case where A is not full rank will be considered below.
- m>n, the solution is the one capable of minimizing the quantity:

  $$\|b - Ay\|$$

  That is, in this case there are more constraints than free variables y. Hence, it is generally impossible to find a solution to these equations. This pseudo-inverse gives the solution y, so that $A^{\intercal}$y is closest (in a LS (Least Squared) sense) to the desired solution for vector b.

- m<n, then the Moore-Penrose solution minimizes the 2-norm of y:$\|y\|$. In this case, there exists, generally, an infinite number of acceptable solutions, and the Moore-Penrose solution is the particular solution in which the vector 2-norm is minimal.

However, when A is not full rank, then these formulas cannot be used [57].